Uptake and release of metal ions by transferrin and interaction with receptor 1

ARTICLE *in* BIOCHIMICA ET BIOPHYSICA ACTA · AUGUST 2011

Impact Factor: 4.66 · DOI: 10.1016/j.bbagen.2011.07.008 · Source: PubMed

3 AUTHORS, INCLUDING:

Miryana Hémadi
French National Centre for Scientific Research
25 PUBLICATIONS **375** CITATIONS
SEE PROFILE

Ha Duong Thanh
Paris Diderot University
21 PUBLICATIONS **328** CITATIONS
SEE PROFILE

Uptake and release of metal ions by transferrin and interaction with receptor 1

Jean-Michel El Hage Chahine, Miryana Hémadi, Nguyêt-Thanh Ha-Duong

PII: S0304-4165(11)00174-7
DOI: doi: 10.1016/j.bbagen.2011.07.008
Reference: BBAGEN 27058

To appear in: *BBA - General Subjects*

Received date: 29 April 2011
Revised date: 12 July 2011
Accepted date: 13 July 2011

Please cite this article as: Jean-Michel El Hage Chahine, Miryana Hémadi, Nguyêt-Thanh Ha-Duong, Uptake and release of metal ions by transferrin and interaction with receptor 1, *BBA - General Subjects* (2011), doi: 10.1016/j.bbagen.2011.07.008

Highlights

Interaction of metal-loaded transferrins with Receptor-1
Metal release from the transferrin/receptor-1 adduct in the cell
Ultra fast interaction of the C-lobe of metal-loaded transferrin with the helical domain of receptor 1
Metal endocytosis occurs mainly with the C-lobe of transferrin interacting with the helical domain of receptor-1

Uptake and Release of Metal ions by Transferrin and Interaction with Receptor 1

Jean-Michel El Hage Chahine*, Miryana Hémadi and Nguyêt-Thanh Ha-Duong

Université Paris Diderot Sorbonne Paris Cité – CNRS, Interfaces, Traitements, Organisation et Dynamique des Systèmes – UMR 7086 ; Bâtiment Lavoisier, 15 rue Jean-Antoine de Baïf, 75205 Paris Cedex 13, France

* To whom correspondence should be addressed.
Tel: 33157277238
Fax: 33157277263
E-mail: chahine@univ-paris-diderot.fr

Keywords. Iron-acquisition pathway, protein/protein interactions, cobalt, uranium, aluminum.

Abbreviations. T, apotransferrin; T_C, the C-lobe of apotransferrin in an unknown state of charge and protonation; T_CFe, C-site-loaded monoferric transferrin; TFe_2, TAl_2, TGa_2, TCo_2, TBi_2, metal-saturated transferrins; Ur, uranyl (UO_2^{2+}); TUr_2, uranyl-saturated transferrin; TFR, transferrin receptor 1 subunit; TFR_a, the acidic form of TFR; TFR -TFe_2, -TGa_2, -TCo_2, -TBi_2, metal-loaded transferrin-receptor 1 protein/protein adduct; NTA, nitrilotriacetate; AHA, acetohydroxamic acid; HFE, hemochromatosis protein.

Abstract.

Background For a metal to follow the iron-acquisition pathway, four conditions are required: 1- complex formation with transferrin; 2- interaction with Receptor-1; 3- metal release in the endosome; 4- metal transport to cytosol.

Scope of the review This review deals with the mechanisms of aluminum(III), cobalt(III), uranium(VI), gallium(III) and bismuth(III) uptake by transferrin and interaction with receptor 1.

Major conclusions The interaction of the metal-loaded transferrin with receptor 1 takes place in one or two steps: a very fast first step (μs to ms) between the C-lobe and the helical domain of the receptor, and a second slow step (2–6 hours) between the N-lobe and the protease-like domain. In transferrin loaded with metals other than iron, the dissociation constants for the interaction of the C-lobe with TFR are in a comparable range of magnitudes 10 to 0.5 μM, whereas those of the interaction of the N-lobe are several orders of magnitudes lower or not detected. Endocytosis occurs in minutes, which implies a possible internalization of the metal-loaded transferrin with only the C-lobe interacting with the receptor.

General significance A competition with iron is possible and implies that metal internalization is more related to kinetics than thermodynamics. As for metal release in the endosome, it is faster than the recycling time of transferrin, which implies its possible liberation in the cell.

The transport and incorporation of metals other than iron by transferrins is a very intriguing tale indeed. Human serum-transferrin is known to form stable complexes with more than forty metallic cations, which include transition metals, actinides and metals of group 13 of the periodic table [1-3]. However, as attractive as this hypothesis may sound, we should always keep in mind that transferrin is a metal solubilizer in the blood stream and that, alone, it cannot transport iron to its targets inside the cells [4]. In order to do so, the metal-loaded transferrin needs to interact mainly with transferrin receptor 1 or, to a lesser extent, with receptor 2 [5-7]. The interaction with the receptor leads to the endocytosis of the transferrin/receptor adduct in the cytosol [6]. The endosomes formed then undergo a drop in their inner pH, which leads to the release of iron, or eventually other metals, from the protein/protein adduct, to the reduction of Fe(III) to Fe(II) and to its active transport from the endosome to its targets in the cell [6, 8-9]. The endosome is recycled back to the plasma membrane, where transferrin is released in the neutral biological fluid ready for a new iron-acquisition cycle [6]. Therefore, it can easily be assumed that the formation of a stable complex between a metal and transferrin is only one of several steps involved in its possible transport by the iron-acquisition pathway.

We shall deal here with the mechanisms of iron, cobalt, bismuth, aluminum, gallium and uranium uptake by human serum-transferrin (T) and with the interactions of the metal-loaded transferrins with receptor 1 [4, 10-15]. We shall also deal with the mechanism of iron release in vitro from the holotransferrin (TFe_2)/receptor 1 adduct in acidic media and transpose this process to metals other than iron [16].

The structures of human serum-transferrin (T) and receptor 1 were reported and analyzed in this issue by K. Mizutami. They will, therefore, not be developed further here. However, we should remind the reader that transferrin is a glycoprotein of 700 aminoacids organized in two semi-equivalent lobes, each of which contains an iron-binding site composed of two phenols

of two tyrosines, a carboxylate of an aspartate, an imidazole of a histidine and a synergistic carbonate adjacent to an arginine. Earlier studies, by X-ray solution scattering and more recently the crystal structure of the protein led to the conclusion that the apo (iron-free) and holo (iron-saturated) forms of transferrin exist for the majority of the time in well-defined specific conformations representing a "fully-opened" and "closed" states, respectively [17]. In the open conformation of the apoform of transferrin, the protein ligands are in direct contact with the bulk medium. When it is iron-loaded, each lobe encloses the coordinated metal, which becomes buried about 10 Å under the surface of the protein in the closed conformation (Scheme I) [18-19].

Receptor 1 is a 190 kDa homodimeric protein arranged in two subunits (TFR) linked by two disulfide bridges. The receptor contains a transmembrane domain, a cytoplasmic endodomain of about 15 kDa and a soluble ectodomain directed towards the biological fluid. The ectodomain is arranged in three domains: the helical, the apical and the protease-like, which forms a pseudo-cavity of about 10 Å with the plasma membrane [20]. The endodomain consists of a transmembrane segment and a cytosolic part. The C-lobe of holotransferrin (TFe_2) or that of a C-lobe-only iron-loaded transferrin interacts with the helical domain, whereas the N-lobe interacts with protease-like domain in the cavity with the plasma membrane [21].

As written above, the first step in the iron-acquisition pathway is the formation of a complex between Fe(III) and T. Fe(III) is almost insoluble in aqueous neutral media, where it readily precipitates as different iron hydroxides [22]. Fe(III) is usually solubilized under the form of chelates or complexed to proteins or macromolecules. In the bloodstream, of normal individuals practically all the circulating iron is complexed to transferrin and another infinitesimal part is complexed to ceruloplasmin [23]. It is generally accepted that in the normal individual about 0.1% of the total body iron (i.e. about 3 to 4 mg) is in the plasma,

bound predominantly to transferrin (which is approximately 30% saturated with iron). The daily turnover of iron is about 30 mg, so transferrin is continually binding iron (both dietary and "recycled" iron) and delivering it to cells and tissues. [9, 22].

Ceruloplasmin (Cp) is a blood-circulating protein, which plays a major role in iron and copper homeostasis [24-25]. More than 95 % of the copper in the plasma is bound to Cp, which also possesses two iron-binding sites [23]. Cp is, in addition, one of the major ferroxidases involved in the Fe(II) to Fe(III) oxidation.

Transferrin forms complexes with Fe(III) and lacks any significant affinity for Fe(II), which is readily oxidized in aerobic media [26]. How, then, is iron acquired by transferrin? Several possibilities are envisaged. We shall only report two. The first is required for the understanding of the uptake of metals other than iron by transferrin. It concerns metal transfer from the so-called low-molecular-weight iron pool to transferrin. This iron pool is assumed to consist of undetectable concentrations of iron(III) complexed to low mass chelators (FeL)[9]. The second very interesting theory assumes that iron(III) is transferred from ceruloplasmin to transferrin, after the oxidation of iron(II), in a protein/protein adduct formed by the interaction of the two proteins (Scheme II) [27]. This hypothesis shall not be further discussed here.

1. Metal transfer from a low-molecular-mass chelate to transferrin

The mechanisms of iron and metal transfer from chelate to transferrin proposed here are those we have established since the mid-nineties, essentially by means of the methods and techniques of fast kinetics associated with spectrophotometric detection and titration. Apotransferrin (T), transferrin with only its C-site iron-loaded (T_CFe) and holotransferrin (TFe_2) have specific absorption and intrinsic emission spectra (Figure 1)[28], which makes it possible to follow the kinetics of iron uptake by spectrophotometric techniques. In earlier observations, based on stopped-flow mixing associated with absorption spectroscopy, Bates

and coworkers showed that iron can be very rapidly extracted by transferrin from low-mass chelates, such as Fe(III)nitrilotriacetate (FeNTA) or Fe(III)acetohydroxamate (FeAHA) [29-30]. These observations were afterwards completed and extended to lactoferrin and ovotransferrin [15, 31-33]. This approach was also applied to other metal chelates, such as aluminum citrate, bismuth nitrilotriacetate, gallium nitrilotriacetate, cobalt nitrilotriacetate-carbonate and uranyl carbonate [3-4, 10-12, 14]. The stopped-flow apparatus set-up is a fast-mixing device (~ 1 ms) associated with a fast detection technique, such as a spectrophotometer, which allows the analysis of the kinetic processes occurring in the range of milliseconds to the few seconds (Figure 2) [10]. Other, different, approaches were used with several other metals [1-2, 34-39].

1.1 Iron-uptake by transferrin

When a neutral solution of apotransferrin is rapidly mixed with a neutral solution of FeNTA or FeAHA in the presence of bicarbonate, four kinetic processes are detected by fluorescence emission in the 300 to 400 nm range with an excitation wavelength λ_{ex} = 280 nm. The first is fast and occurs in the 0.1 s range as an exponential decrease in fluorescence emission. It is followed by an exponential decrease in the emission, which, however, occurs in the second range. The third and fourth kinetic phenomena take place in the 100 s and the 1000 s range, respectively (Figure 3). The methods of chemical relaxation were used to analyze these kinetic processes and to propose a general mechanism for iron transfer from a chelate to apotransferrin in the presence of bicarbonate [15, 32]. Chemical relaxation is a kinetic approach for the analysis of fast kinetic processes in the fundamental state. It was developed in the sixties by Manfred Eigen and co-workers [40-41].

In neutral physiological media, about 30% the C-lobe of transferrin interacts with bicarbonate, whereas the N-lobe does not [42]. Although transferrin can be found in the blood stream with the N-lobe iron-loaded and the C-lobe iron-free [43], the thermodynamic and kinetic data

(Table 1, eq 1) clearly indicate that the first process in Figure 3A is that of an iron(III) transfer from the chelate to the iron-binding site in the C-lobe of transferrin interacting with the bicarbonate [42]. This process is accompanied by a proton loss and corresponds to a first complex formation between a phenolate of one of the tyrosines and Fe(III). It is immediately followed by a fast change in the conformation of the lobe, leading to a second proton loss and allowing a new coordination between the phenolate of the second tyrosine and the metal (Figure 3 B). During this conformational change, the two domains of the C-lobe start to enclose the metal like a pair of jaws. This process (Figures 3B) triggers another conformational change accompanied by proton losses affecting the whole protein, including the N-lobe, which rate-controls a very fast second iron(III) uptake if the metal is available [32]. It is followed by a final conformational change allowing the C-lobe-only iron-loaded transferrin and/or holotransferrin to achieve its final state of equilibrium (Table 1, eqs 1-11) [15, 32]. During these four processes, the conformation of the protein transits from open for apotransferrin to closed for holotransferrin, where iron is coordinated to the four protein ligands of Scheme I and also completely protected from the outside medium. In this multistep system, the affinity of the C-lobe of protein for iron grows from 10^{16} M^{-1} for the first kinetic intermediate up to about 10^{21} M^{-1}, whereas that of the N-lobe attains 10^{20} M^{-1} [15, 44].

1.2 The role of the donor chelate in metal uptake

Metal uptake by transferrin depends on the nature of the metal-providing chelates, which can roughly be classified in three groups. In the first, as for iron in the case of FeNTA and FeAHA, the metal dissociation is fast and does not rate-control iron uptake [15]. In the second case, as for iron-citrate, it is extremely slow [45-46] and metal-binding becomes rate-controlled by chelate dissociation [15, 45]. There is also a third case, which will be developed further. In this latter, the chelate is either a mixed complex already containing the carbonate ligand, such as $CoNTACO_3^{2-}$ or a tricarbonate complex, such as $UO_2(CO_3)_3^{4-}$ [11, 47].

1.3 Aluminum, gallium and bismuth uptake by transferrin

In Table 1, we summarize the mechanisms of metal transfer from FeNTA, FeAHA, Al(III)citrate, Ga(III)nitrilotriacetate and Bi(III)nitrilotriacetate to transferrin. All these chelates seem to dissociate quite rapidly and their dissociation does not rate-control metal uptake by transferrin. When a solution of each of them is mixed, by stopped-flow, with T in the presence of HCO_3^-, three kinetic processes are detected by spectrophotometric absorption or emission monitoring in, however, extremely different time ranges. They resemble those observed for iron uptake (Figure 3) and will not, therefore, be reproduced here [4, 10, 14]. The first is ascribed to metal transfer from the chelate to the C-lobe iron-binding site (Table 1, eqs 12, 20, 28). The second and third are ascribed to conformational change affecting the whole protein and rate-controlling metal uptake by the N-lobe binding site (Table 1, eqs 3-11, 13-19, 21-27, 29-31).

These processes are fast for bismuth, where they occur in less than 100 ms for metal transfer from chelate to the C-lobe binding site, and less than 0.5 and 50 s for the second and third conformational changes, respectively [14]. With aluminum and gallium, the time ranges vary from about 50 seconds for the first and 1000 and 60000 seconds for the two following processes [4, 10]. This clearly implies that bismuth transfer from BiNTA to transferrin occurs very rapidly and that the Bi-loaded protein attains it final equilibrated state in a few seconds (Table 1). This occurs with high affinities ($10^{18} \sim 10^{19}$ M^{-1}) despite the ionic radius of Bi^{3+} (1.03 Å) and the suspected structure of the Bi-loaded transferrin in which the lobes are in a semi-closed conformation with bismuth in partial contact with the bulk medium [14, 48]. With bismuth citrate, Bi(III)-uptake is slowed down to several hours [48]. This, again, underlines the important role played by the rate of chelate dissociation in metal uptake by transferrin. With gallium and aluminum, metal transfer becomes rather slow and the final equilibrium is only attained after several hours [4, 10].

1.4 Why metal uptake first occurs by the C-lobe binding site?

Metal uptake by transferrins requires a synergistic anion, without which it does not occur [31, 49-51]. The naturally occurring synergistic anion is HCO_3^-, which is involved in the buffering of natural media [50, 52]. However, in vitro and with some bacterial transferrins, several anions can play such a role [49-50, 53-56]. On the other hand, in physiological media, 30% of the C-lobe of T is in interaction with HCO_3^-, whereas the N-lobe hardly interacts with the synergistic anion (Table 1, eq 1)[31, 42, 51]. Furthermore, in holotransferrin, a carbonate, adjacent to an arginine, is a part of the coordination sphere of the metal [57]. Therefore, the presence of HCO_3^- in the C-lobe of transferrin should considerably facilitate the first step in the coordination to the metal [31, 51]. This step is accompanied by three proton losses, one from the bicarbonate and the two others from the phenols of the tyrosines (Table 1) [32, 44, 52, 58]. This can also explain the close similarities between the mechanisms of metal transfers to T from Al(III), Bi(III) and Ga(III) chelates and that of Fe(III). Indeed, all occur first with the binding site in the C-lobe and then with that in the N-lobe (Table 1). What can now happen if the metal-providing chelate has carbonate as a ligand?

1.5. Uranyl and Cobalt uptake by transferrin from uranyl tricarbonate and the mixed Co(III)carbonate nitrilotriacetate complex

In Table 2, we summarize the mechanisms of uranyl and cobalt uptake by transferrin. Uranium(VI) exists in biological media mainly as uranyl (Ur), UO_2^{2+} [37, 59-61]. When present in sera, in the case of exposure or contamination, Ur exists in the form of the tricarbonate and dicarbonate complexes (eq 32) [60, 62]. It is also complexed to other circulating proteins but, mainly to transferrin [37, 47, 59, 61, 63-64]) :

$$Ur(CO_3)_3^{4-} + H^+ \rightleftharpoons Ur(CO_3)_2^{2-} + HCO_3^- \quad \text{(fast)} \quad (32)$$

When a solution of apotransferrin is mixed with a solution of Ur in the presence of HCO_3^-, four kinetic processes are detected (Figure 4). The first is very fast and occurs in the tens of

milliseconds range as an exponential decrease in fluorescence to yield a first kinetic product (Figure 4A). The latter yields another kinetic product in a process, which appears as an exponential decrease of the emission occurring in the range of a second (Figure 4B). These two processes are followed by two other kinetic phenomena during which the Ur-saturated T attains its thermodynamic state of equilibrium (Figure 4C). The third is an exponential increase in absorption in tens of minutes. It is followed by an increase in absorption lasting about six hours. We recently showed that only the tricarbonate complex is responsible for the fast formation of the first ternary complex with the C-lobe of transferrin accompanied by bicarbonate loss (eq 33).

$$Ur(CO_3)_3^{4-} + T_C \underset{k_{-1}}{\overset{k_1}{\rightleftharpoons}} (T_CUr(CO_3)_2)' + HCO_3^- \quad \text{(rate-limiting)} \qquad (33)$$

where T_C is the C-lobe of transferrin in an unknown sate of protonation and $(T_CUr(CO_3)_2)'$ is a kinetic ternary complex intermediate in an unknown state of protonation; k_1 and k_{-1}, the elementary second-order rate constants [47].

This ternary complex undergoes a change in conformation (eq 34) accompanied by a second bicarbonate loss to produce a second kinetic product (eq 35), in which only the C-lobe of transferrin is uranyl-loaded.

$$(T_CUr(CO_3)_2)' \underset{k_{-2}}{\overset{k_2}{\rightleftharpoons}} (T_CUr(CO_3)_2)'' \quad \text{(rate-limiting)} \qquad (34)$$

$$T_CUr + HCO_3^- \rightleftharpoons (T_CUr(CO_3)_2)'' \qquad (35)$$

with T_CUr, a C-lobe uranyl-loaded transferrin intermediate.

These two processes initiate a series of slow to very slow conformational changes (Table 2, eqs 36). They affect the whole transferrin, including the N-lobe, and allow the N-binding site to complex a second uranyl. The first process in uranyl uptake by transferrin is faster than that observed with iron because the synergistic anion is provided by the metal/donor complex. As

for the slowest steps, they seem to be quite similar with, however, rates different from those observed for the uptake of other metals, such as iron, aluminum, bismuth and gallium (Tables 1 and 2)[4, 10, 14-15, 47].

A multi-process system is also observed for cobalt uptake from the mixed nitrilotriacetate carbonate complex $CoNTACO_3^{2-}$. Here the first step becomes much too fast for a stopped-flow detection. It was detected by the temperature-jump technique (T-jump). T-jump is based on Joule heating by the discharge of a capacitor through the solution. Heating times can be as low as 200 ns and heating amplitudes as high as 12 °C. This technique allows us to deal with kinetic runs occurring in the µs to ms range (Figure 5) [11, 40-41]. In our case, the detection was based on the variations in absorption or fluorescence emission (Figure 6) [11]. The first step in the cobalt-transferrin complex formation occurs in less than 2 ms. It corresponds to a $CoCO_3^+$ transfer from the mixed $CoNTACO_3^{2-}$ complex to the C-lobe of transferrin (eq 37):

$$T_CH_m + CoNTACO_3^{2-} \underset{k_{-3}}{\overset{k_3}{\rightleftharpoons}} T_CH_mCoCO_3 + NTA^{3-} \qquad (37)$$

with T_CH_m, the C-lobe with all ligands protonated in an unknown state.

This first process is followed by three slower processes lasting from about 50 seconds to more than 24 hours, during which the first kinetic product undergoes a series of proton losses triggering conformational changes similar to, but however slower, than those observed for iron. These changes allow the N-site to complex in turn a second cobalt (Table 2, eqs 38-40)[11].

1.6 Some general considerations about metal uptake by transferrin

Analysis of the mechanisms in Tables 1 and 2 clearly shows that, apart from the case of the mixed carbonate or carbonate complexes, the first step in metal uptake is that of the interaction of the C-lobe of the protein with HCO_3^- . In serum ($[HCO_3^-]$ ~ 20 – 25 mM), we have already mentioned that the C-lobe and an insignificant part of the N-lobe are interacting with bicarbonate [42]. This renders the N-lobe much less reactive than the C-lobe towards

metal uptake. Nevertheless, metal transfer from the chelate to the C-lobe leads to a series of events, mainly conformational changes, triggered by proton losses from the protein ligands and from some aminoacids situated in each of the two domains that surround the binding cleft in each lobe. These proton losses produce a sort of a zipping effect, which allows the protein ligands to complex the metal and interdomain hydrogen bonding to occur [65]. This initiates the indispensible changes in conformation which bring the ligands close to the metal. This subsequently leads to the transition from the open structure, in which the ligands are in contact with the bulk medium, to the closed structure, in which the ligands are engaged in the complex and the metal is enclosed in the binding cleft (Scheme I) [15, 65-68], This case is, however, quite different with at least three metallic cations, Al^{3+}, Bi^{3+} and UO_2^{2+}. Indeed, in these cases metal-loaded transferrin is assumed to be in a semi-closed conformation in which the metal is not fully included in the binding clefts of the two lobes and, thus, partly in contact with bulk medium [59, 61, 69-70]. This can explain the comparatively low affinities of the protein for aluminum or uranyl, but not the high affinity for bismuth [1-2, 59, 61, 69-70].

2. Interaction of metal-loaded transferrins with receptor 1

Aluminum, bismuth, gallium cobalt and uranyl form stable complexes with transferrin [1-2, 70], but in sera, aluminum is partly complexed to citrate and uranyl is shared between the carbonate and to a lesser extent the transferrin complexes. In contrast, bismuth, gallium and cobalt are mainly complexed to transferrin [1-2, 27, 37, 59-60, 69]. Therefore, transferrin can be involved in these metals transport system in serum. However, is it involved in their incorporation into cells? To partly answer this question, we analyzed, in vitro and in the presence or absence of CHAPS micelles, the interaction of the metal-loaded transferrins with the full non-cleaved receptor 1. Henceforth and for reasons of simplicity, we shall only refer to the receptor 1 subunit (TFR). CHAPS micelles play the role of artificial membranes which solubilize the trans-membrane domain of the receptor and allow its monodisperse presence in

the medium in a non-aggregated fashion [3-4, 10-14, 71]. The following analysis is based on two different approaches: 1) thermodynamics and 2) kinetics.

2.1 Thermodynamics of protein/protein interaction between iron-saturated transferrin and receptor 1

In neutral media, receptor 1 exists as two prototropic species (eq 41) with a K_a of 10 nM [13].

$$TFR + H^+ \rightleftharpoons TFRH \qquad (41)$$

$$K_a = [TFR][H^+]/[TFRH]$$

Spectrophotometric titration monitored by fluorescence emission showed that TFR interacts with TFe_2 and not with T. The overall dissociation constant involved in this protein/protein adduct was measured in neutral media (eq 42). It showed a very strong interaction between the two proteins (K_{d2} = 2.3 nM) [4].

$$TFR + TFe_2 \rightleftharpoons \text{un-identified steps} \rightleftharpoons TFRTFe_2 \qquad (42)$$

with $K_{d2} = [TFR][TFe_2]/[TFRTFe_2]$.

These results were acquired at the final equilibrated state and do not give any information about the mechanism of the interactions between TFe_2, and the receptor. A kinetic investigation was therefore, undertaken.

2.2 Kinetics of protein/protein interaction between iron-loaded transferrin and receptor1

When a solution of TFe_2 and TFR solubilized by CHAPS micelles is submitted to a fast T-jump from 25 to about 37 °C, two very fast kinetic processes are observed (Figure 2A). The first occurs in less than 1 µs and corresponds to the interaction of the receptor with the CHAPS micelles. It is followed by another process occurring in the tens of µs range, which corresponds to an interaction between the receptor and TFe_2. This process is followed by a very slow phenomenon (about 2 hours), during which the protein/protein adduct attains its thermodynamic equilibrated state (Figures 7, 8). The first process is not observed in the absence of the CHAPS micelles, whereas the second and third are still detected with,

however, a low signal-to-noise ratio. The fastest process detected is, therefore, ascribed to the dissociation of the CHAPS micelles, which does not interfere with the forthcoming kinetic events [13]. Subsequently, the interaction of TFe_2 with TFR occurs in two sequential steps: I) a very fast process, which leads to a kinetic intermediate protein/protein adduct with a dissociation constant, K_{d1} of 0.5 µM, II) a slow conformational change of the intermediate, which produces the thermodynamic $TFRTFe_2$ complex. This process stabilizes the protein/protein adduct by a factor of about 300 and leads to the overall K_{d2} of 2.3 nM reported above [13]. Cheng et al. showed that the interaction of the C-lobe of TFe_2 is strong, and occurs with the helical domain of the receptor, whereas that of the N-lobe is weak, and occurs in the cavity formed between the protease-like domain and the plasma membrane [21]. The first strong interaction depicted by the fast kinetic process is, thus, related to the interaction of the C-lobe of TFe_2 with the helical domain of TFR, whereas the second slow and weak interaction is due to a conformation change allowing the N-lobe to interact with the protease-like domain (Figures 7 and 8, Table 3, eqs 43,44) [14, 16].

2.3 The case of aluminum, bismuth, gallium, cobalt and uranium

In vitro, no interaction between TAl_2 and TFR is detected. This, however, does not imply its absence. It only indicates that this interaction is either much too weak to be detected by fluorescence emission, or that it does not lead to sufficient variation in the emission spectra to allow detection [4]. TBi_2, TGa_2, TCo_2 and TUr_2 interact with TFR [3, 47]. However, these interactions are not always similar to those reported for iron. Indeed, the overall dissociation constants involved vary from 2.3 nM for iron, to 6 µM for uranyl and is undetected for aluminum (Table 3) [3-4, 12]. Furthermore, the mechanisms of interactions between the metal-loaded transferrin and TFR can differ from those reported for TFe_2. Indeed, TBi_2 and TGa_2 interact with TFR in a single kinetic step similar to that attributed to the interaction of the C-lobe of TFe_2 with the helical domain, with no second step related to the interaction of

the N-lobe with the protease-like domain. The rate constants and half-lives involved also differ considerably (about 20 µs for TFe_2, up to 15 ms for TUr_2; Figure 8, Table 3) [10-12, 14]. Conversely, the behavior of TCo_2 is similar to that of iron with a fast interaction with the C-lobe and a very slow one with the N-lobe (Table 3, Figure 8) [11]. With TUr_2, the two interactions with the C- and N-lobes are fast [12].

3. Metal-loaded transferrins and internalization by the iron-acquisition pathway

Table 3 clearly shows that the overall affinities of metal-loaded transferrins for the receptor as compared to that of TFe_2 are weak to very weak. Apart from TCo_2, this excludes any possible competition between the metal-loaded transferrins and TFe_2 for TFR. However, endocytosis occurs in the minute range [72]. This process is much faster than the interaction of the N-lobe with TFR, which occurs in the hour range, and much slower than that of the C-lobe with TFR, which occurs in the tens of µs range with TCo_2 to the ms range with TUr_2 [11, 47]. Although in the early nineties, experiments performed with rabbit reticulocytes and iron-loaded transferrins led to assume that the affinities of both lobes to the receptor are almost identical [73], it was recently shown that, transferrin in which only the C-lobe is metal-loaded interacts strongly and rapidly with the receptor [3-4, 21]. This implies that metal-loaded transferrins are most probably internalized by endocytosis with mainly their C-lobe interacting with TFR. Surface plasmon resonance was used to obtain kinetic and thermodynamic data related to the interaction of TFe_2 and the hemochromatosis protein HFE with the soluble ectodomain of the receptor (Table 3) and a series of its mutants. It was shown that despite a lower affinity for the ectodomain than TFe_2, HFE blocks the interaction of the latter with the receptor [74-75]. Although our experiments were performed with the complete non-cleaved receptor and by means of the chemical relaxation techniques, it is still possible to compare the mechanisms of these protein/protein interactions. Indeed, TFe_2 interacts with both the helical and the protease-like domains [3, 21], and the overall affinity of holotransferrin for receptor 1 is about

fifty times that of HFE (Table 3) [21, 75]. However, the affinity of the C-lobe for TFR is about fifty times lower than that of HFE [3-4, 21]. Both interactions are instantaneous as compared to that of the N-lobe of TFe_2 with TFR and to endocytosis [3]. Therefore, although the competition between both HFE and TFe_2 for TFR is thermodynamically largely in favor of TFe_2, the interaction of HFE with the helical domain of TFR is, within the time range of endocytosis, much more favored than that of the C-lobe of TFe_2. It can, therefore, perturb the acquisition of iron by receptor-mediated endocytosis. The same reasoning can apply for TCo_2, TBi_2, TGa_2 and TUr_2, where the overall affinity for TFR is lower than that of TFe_2 (Table 3). Nonetheless, the affinities of the C-lobe of these metal-loaded transferrins are of the same order of magnitude as that of TFe_2 for TFR (Table 3). In this case, these metal-loaded transferrins can compete with holotransferrin for TFR and can be internalized to different extents (more for TCo_2 and less for TUr_2) by transferrin receptor-mediated endocytosis [10-14]. With TUr_2, both interactions of the C- and N-lobes occur within the life span of endocytosis, which implies a possible internalization of TUr_2 with both lobes interacting with TFR. However, this last case implies a high concentration of Ur in the serum, which can only be achieved under conditions of severe contamination (exposure to uranium used for civil or military purposes) [47, 76-77]. As interesting as these results may be, they cannot imply that the incorporation of these metals can follow the iron-acquisition pathway. Indeed, in order to do so, the metal should first, be released from the protein/protein adduct in the acidic medium of the endosome.

4. Metal release from transferrin in interaction with receptor 1 in media close to those of the endosome

In acidic media, transferrin receptor 1 exists in an acidic form TFR_a [13, 78]. TFR_a is also present in the mildly acidic medium (pH < 6) of the endosome as two prototropic species (eq 53) with a protodissociation pK_{1a} of 5.6 [13].

$TFR_a + H^+ \rightleftharpoons TFR_aH$ (53)

$K_{1a} = [TFR_a][H^+]/[TFR_aH]$

An interaction occurs between apotransferrin T and TFR_a. This interaction is rate-controlled by a slow (about 20 minutes) conformational change in TFR_a and occurs with an overall dissociation constant, K_{1D} = 36 nM (Table 4, eq 54,55) [13].

$TFR_a \rightleftharpoons TFR'_a$ (rate-limiting) (54)

$TFR'_a + TH_6 \rightleftharpoons TFR_a\text{-}TH_6$ (55)

with $K_{1D} = [TFR_a][TH_6]/[TFR_aTH_6]$ and TH_6, apotransferrin with all protein ligands in the protonated state.

When a neutral solution of TFe_2 interacting with TFR is mixed with a mildly acidic buffer to reach a final pH of 4.5 to 6, three kinetic processes are detected by fluorescence emission (Figure 9) [16]. The first occurs in 0.1 to 0.5 second and corresponds to iron release from the N-lobe interacting with the protease-like domain and is rate-controlled by a conformational change triggered by a proton gain. The second process corresponds to iron-loss from the C-lobe upon interaction with the helical domain. It is rate-controlled by another conformation change, triggered, by another proton gain, and finally the equilibrium depicted by eqs (54) and (55) is attained (Table 4) [16]. Compared to iron loss in the absence of TFR, the interaction with the receptor accelerates iron release in acidic media, even in the absence of a competing ligand such as citrate [16, 65, 79]. During these processes, TFe_2 interacting with TFR undergoes proton-triggered conformational changes, during which each lobe transits from its closed to open conformation by a proton-induced unzipping effect [16, 65, 79]. The first step in this unzipping is proton-assisted decarbonation of the N-lobe-binding cleft and then protonation of the aminoacids engaged at the lips of the cleft, which breaks the interdomain hydrogen-bonds and opens the binding cavity to the bulk medium [65]. This is followed by sequential protonation of the protein ligands, which successively breaks each

coordination bond, finally releasing the metal and allowing the lobe to adopt the open structure. The overall proton gain during iron loss at pH 4.5 to 6 is 3 protons per binding site, with an average pK_a value of 5.3 for the N-lobe and 5.1 for the C-lobe (Table 4, Figure 10) [16]. After losing iron in the endosome, T remains interacting with the acidic form of the receptor and is recycled to the plasma membrane (Table 4) [16]. These results were reported for the non-cleaved transferrin receptor, the transmembrane part of which was solubilized by CHAPS micelles [16]. They are, however, at variance with recent results acquired with the soluble ectodomain of the receptor [80]. Nonetheless, in both approaches, it is estimated that iron is released in the endosome in about 2 minutes. This is short compared to the endocytic cycle which takes several minutes [16, 80].

5. Metal release in the endosome and incorporation by the cell

The structures of the cobalt- and gallium-loaded transferrins seem to be quite close to that of holotransferrin [10-11, 59, 64, 69-70]. In this case iron loss from TGa_2 and TCo_2 would occur by mechanisms similar to those reported in Table 4. However, with normal transferrin, TAl_2 does not seem to interact with the receptor [4], which was explained by the partly open structure of the binding clefts in each of the two lobes [69]. This reduced affinity of T for the metal and that of the metal-loaded transferrin for the receptor was also reported in the case of some abnormal human transferrins [81]. As for TBi_2 and TUr_2, they also appear to be in a semi-open structure where the metal cation is not completely enclosed in the binding cleft and is partly exposed to the bulk medium [59, 64, 70]. This can probably facilitate their release in the endosome. It does not, nevertheless, imply their incorporation by the iron-acquisition pathway, because in order to do so, several other steps are still required. Indeed, iron is transported from the endosome to the cytosol in the +2 oxidation state by divalent metal-transport systems, such as DMT1 [8, 82]. This iron reduction may occur after or before iron release [83-85]. However, U(VI), Bi(III) and Ga(III) do not normally exist in the +2 oxidation

state [70, 86-87]. Does this imply their recycling back to the plasma membrane after completion of the iron-delivery cycle by endocytosis? Or can they be delivered to the cytosol by means other than reduction and active transport through the membrane of the endosome?

Conclusion

Several metals form stable complexes with transferrin. Some of these metal-loaded transferrins are recognized by receptor 1 with, however, lower affinities than that of TFe_2. Nonetheless, in iron delivery by the transferrin-receptor-mediated iron acquisition pathway, the essential step is the interaction of the C-lobe of the metal-loaded T with the helical domain of the receptor. Indeed, this interaction is instantaneous, strong and much faster than endocytosis. On the other hand, the interaction of the N-lobe of the protein with the protease-like domain of the receptor is weak or nonexistent and much slower than endocytosis. It is therefore not much involved in the internalization process. This implies that metal-loaded transferrins such as TCo_2, TBi_2, TUr_2 and TGa_2 or other proteins such as HFE, which possess lower overall affinities for receptor 1 than TFe_2, but comparable or higher affinities than TFe_2 for the helical domain of receptor 1 can compete with TFe_2 and possibly be internalized by receptor-mediated endocytosis. This, however, does not imply that their incorporation necessarily takes place by the iron-acquisition pathway, because iron is transported from the endosome to the cytosol by a divalent metal transporter in the 2+ oxidation sate. Beside iron, only and cobalt can achieve such a goal.

References

[1] W.R. Harris, Equilibrium constants for the complexation of metal ions by serum transferrin, Adv Exp Med Biol, 249 (1989) 67-93.
[2] H. Sun, H. Li, P.J. Sadler, Transferrin as a metal ion mediator, Chem Rev, 99 (1999) 2817-2842.
[3] N.T. Ha-Duong, M. Hemadi, Z. Chikh, J.M. Chahine, Kinetics and thermodynamics of metal-loaded transferrins: transferrin receptor 1 interactions, Biochem Soc Trans, 36 (2008) 1422-1426.
[4] M. Hemadi, G. Miquel, P.H. Kahn, J.M. El Hage Chahine, Aluminum exchange between citrate and human serum transferrin and interaction with transferrin receptor 1, Biochemistry, 42 (2003) 3120-3130.
[5] P. Brissot, M.B. Troadec, E. Bardou-Jacquet, C. Le Lan, A.M. Jouanolle, Y. Deugnier, O. Loreal, Current approach to hemochromatosis, Blood Rev, 22 (2008) 195-210.
[6] A. Dautry-Varsat, A. Ciechanover, H.F. Lodish, pH and the recycling of transferrin during receptor-mediated endocytosis, Proc Natl Acad Sci U S A, 80 (1983) 2258-2262.
[7] V.N. Subramaniam, L. Summerville, D.F. Wallace, Molecular and cellular characterization of transferrin receptor 2, Cell Biochem Biophys, 36 (2002) 235-239.
[8] P. Aisen, C. Enns, M. Wessling-Resnick, Chemistry and biology of eukaryotic iron metabolism, Int J Biochem Cell Biol, 33 (2001) 940-959.
[9] R. Crichton, Iron metabolism from molecular mechanisms to clinical consequences, 3rd edition ed., J.Wiley & Sons, Chichester, 2009.
[10] Z. Chikh, N.T. Ha-Duong, G. Miquel, J.M. El Hage Chahine, Gallium uptake by transferrin and interaction with receptor 1, J Biol Inorg Chem, 12 (2007) 90-100.
[11] Z. Chikh, M. Hemadi, G. Miquel, N.T. Ha-Duong, J.M. El Hage Chahine, Cobalt and the iron acquisition pathway: competition towards interaction with receptor 1, J Mol Biol, 380 (2008) 900-916.
[12] M. Hemadi, N.T. Ha-Duong, S. Plantevin, C. Vidaud, J.M. El Hage Chahine, Can uranium follow the iron-acquisition pathway? Interaction of uranyl-loaded transferrin with receptor 1, J Biol Inorg Chem, 15 (2010) 497-504.
[13] M. Hemadi, P.H. Kahn, G. Miquel, J.M. El Hage Chahine, Transferrin's mechanism of interaction with receptor 1, Biochemistry, 43 (2004) 1736-1745.
[14] G. Miquel, T. Nekaa, P.H. Kahn, M. Hemadi, J.M. El Hage Chahine, Mechanism of formation of the complex between transferrin and bismuth, and interaction with transferrin receptor 1, Biochemistry, 43 (2004) 14722-14731.
[15] R. Pakdaman, F.B. Bou Abdallah, J.M. El Hage Chahine, Transferrin, is a mixed chelate-protein ternary complex involved in the mechanism of iron uptake by serum-transferrin in vitro?, J Mol Biol, 293 (1999) 1273-1284.
[16] M. Hemadi, N.T. Ha-Duong, J.M. El Hage Chahine, The mechanism of iron release from the transferrin-receptor 1 adduct, J Mol Biol, 358 (2006) 1125-1136.
[17] J.G. Grossmann, J.B. Crawley, R.W. Strange, K.J. Patel, L.M. Murphy, M. Neu, R.W. Evans, S.S. Hasnain, The nature of ligand-induced conformational change in transferrin in solution. An investigation using X-ray scattering, XAFS and site-directed mutants, J Mol Biol, 279 (1998) 461-472.
[18] J. Wally, P.J. Halbrooks, C. Vonrhein, M.A. Rould, S.J. Everse, A.B. Mason, S.K. Buchanan, The crystal structure of iron-free human serum transferrin provides insight into inter-lobe communication and receptor binding, J Biol Chem, 281 (2006) 24934-24944.
[19] H.J. Zuccola, The crystal structure of monoferric human serum transferrin, Ph. D. Thesis, Ann Arbor, 1992.

[20] C.M. Lawrence, S. Ray, M. Babyonyshev, R. Galluser, D.W. Borhani, S.C. Harrison, Crystal structure of the ectodomain of human transferrin receptor, Science, 286 (1999) 779-782.
[21] Y. Cheng, O. Zak, P. Aisen, S.C. Harrison, T. Walz, Structure of the human transferrin receptor-transferrin complex, Cell, 116 (2004) 565-576.
[22] R.J. Ward, Y. Zhang, R.R. Crichton, Aluminium toxicity and iron homeostasis, J Inorg Biochem, 87 (2001) 9-14.
[23] P.F. Lindley, G. Card, I. Zaitseva, V. Zaitzev, B. Reinhammar, E. Selin-Lindgren, K. Yoshida, An X-ray structural study of ceruloplasmin in relation to ferroxidase activity, J Biol Inorg Chem, 2 (1997) 454-463.
[24] M. Arredondo, M.T. Nunez, Iron and copper metabolism, Mol Aspects Med, 26 (2005) 313-327.
[25] N.E. Hellman, S. Kono, G.M. Mancini, A.J. Hoogeboom, G.J. De Jong, J.D. Gitlin, Mechanisms of copper incorporation into human ceruloplasmin, J Biol Chem, 277 (2002) 46632-46638.
[26] D.C. Harris, P. Aisen, Facilitation of Fe(II) autoxidation by Fe(3) complexing agents, Biochim Biophys Acta, 329 (1973) 156-158.
[27] N.T. Ha-Duong, C. Eid, M. Hemadi, J.M. El Hage Chahine, In vitro interaction between ceruloplasmin and human serum transferrin, Biochemistry, 49 (2010) 10261-10263.
[28] S.S. Lehrer, Fluorescence and absorption studies of the binding of copper and iron to transferrin, J Biol Chem, 244 (1969) 3613-3617.
[29] G.W. Bates, J. Wernicke, The kinetics and mechanism of iron(3) exchange between chelates and transferrin. IV. The reaction of transferrin with iron(3) nitrilotriacetate, J Biol Chem, 246 (1971) 3679-3685.
[30] R.E. Cowart, N. Kojima, G.W. Bates, The exchange of Fe3+ between acetohydroxamic acid and transferrin. Spectrophotometric evidence for a mixed ligand complex, J Biol Chem, 257 (1982) 7560-7565.
[31] F. Bou Abdallah, J.M. El Hage Chahine, Transferrins. Hen ovo-transferrin, interaction with bicarbonate and iron uptake, Eur J Biochem, 258 (1998) 1022-1031.
[32] R. Pakdaman, J.M. El Hage Chahine, A mechanism for iron uptake by transferrin, Eur J Biochem, 236 (1996) 922-931.
[33] R. Pakdaman, M. Petitjean, J.M. El Hage Chahine, Transferrins--a mechanism for iron uptake by lactoferrin, Eur J Biochem, 254 (1998) 144-153.
[34] W.R. Harris, Thermodynamic binding constants of the zinc-human serum transferrin complex, Biochemistry, 22 (1983) 3920-3926.
[35] W.R. Harris, L.J. Madsen, Equilibrium study on the binding of cadmium(II) to human serum transferrin, Biochemistry, 27 (1988) 284-288.
[36] W.R. Harris, L. Messori, A comparative study of aluminum(III), gallium(III), indium(III) and thallium(III) binding to human serum transferrin, Coord Chem Rev, 228 (2002) 237-262.
[37] S. Scapolan, E. Ansoborlo, C. Moulin, C. Madic, Uranium(VI)-transferrin system studied by time-resolved laser-induced fluorescence, Rad Prot Dos, 79 (1998) 505-508.
[38] H. Sun, M.C. Cox, H. Li, A.B. Mason, R.C. Woodworth, P.J. Sadler, [1H,13C] NMR determination of the order of lobe loading of human transferrin with iron: comparison with other metal ions, FEBS Lett, 422 (1998) 315-320.
[39] A.D. Tinoco, E.V. Eames, A.M. Valentine, Reconsideration of serum Ti(IV) transport: albumin and transferrin trafficking of Ti(IV) and its complexes, J Am Chem Soc, 130 (2008) 2262-2270.
[40] M. Eigen, L. DeMaeyer, Relaxation methods, in: S.L. Friess, E.S. Lewis, A. Weissberger (Eds.) Techniques of organic chemistry - Investigation of rates and mechanism of reactions, part II, vol. 8, Wiley Intersciences, New York, 1963, pp. 895-1029.

[41] M. Eigen, Nobel Lecture, (1967).
[42] L. Bellounis, R. Pakdaman, J.M. El Hage Chahine, Apotransferrin proton dissociation and interactions with hydrogencarbonate in neutral media, J Phys Org Chem, 9 (1996) 111-118.
[43] J. Williams, K. Moreton, The distribution of iron between the metal-binding sites of transferrin human serum, Biochem J, 185 (1980) 483-488.
[44] P. Aisen, Transferrin, the transferrin receptor, and the uptake of iron by cells, in: Iron transport and storage in microorganisms, plants and animals, vol. 35, Marcel Dekker, New York, 1998, pp. 585-631.
[45] G.W. Bates, C. Billups, P. Saltman, The kinetics and mechanism of iron (3) exchange between chelates and transferrin. I. The complexes of citrate and nitrilotriacetic acid, J Biol Chem, 242 (1967) 2810-2815.
[46] G.T. Spiro, G. Bates, P. Saltman, The hydrolytic polymerization of ferric citrate II. The influence of excess citrate, J Am Chem Soc, 89 (1967).
[47] M. Hemadi, N.T. Ha-Duong, J.M. El Hage Chahine, Can uranium be transported by the iron-acquisition pathway? Ur uptake by transferrin, J Phys Chem B, (2011).
[48] H. Li, P.J. Sadler, H. Sun, Unexpectedly strong binding of a large metal ion (Bi3+) to human serum transferrin, J Biol Chem, 271 (1996) 9483-9489.
[49] G.W. Bates, A.A. Foley, The influence of inorganic anions on the formation and stability of Fe3+-transferrin-anion complexes, Biochim Biophys Acta, 965 (1988) 154-162.
[50] M.R. Schlabach, G.W. Bates, The synergistic binding of anions and Fe3+ by transferrin. Implications for the interlocking sites hypothesis, J Biol Chem, 250 (1975) 2182-2188.
[51] R. Pakdaman, J.M. El Hage Chahine, Transferrin--interactions of lactoferrin with hydrogen carbonate, Eur J Biochem, 249 (1997) 149-155.
[52] G.W. Bates, G. Graham, Carbonate: key to transferrin chemistry, Adv Exp Med Biol, 74 (1976) 400-407.
[53] S. Dhungana, D.S. Anderson, T.A. Mietzner, A.L. Crumbliss, Phosphate ester hydrolysis is catalyzed by a bacterial transferrin: potential implications for in vivo iron transport mechanisms, J Inorg Biochem, 98 (2004) 1975-1977.
[54] S. Dhungana, D.S. Anderson, T.A. Mietzner, A.L. Crumbliss, Kinetics of iron release from ferric binding protein (FbpA): mechanistic implications in bacterial periplasm-to-cytosol Fe3+ transport, Biochemistry, 44 (2005) 9606-9618.
[55] S. Dhungana, C.H. Taboy, D.S. Anderson, K.G. Vaughan, P. Aisen, T.A. Mietzner, A.L. Crumbliss, The influence of the synergistic anion on iron chelation by ferric binding protein, a bacterial transferrin, Proc Natl Acad Sci U S A, 100 (2003) 3659-3664.
[56] J.M. El Hage Chahine, D. Fain, The mechanism of iron transferrin interactions. Uptake of the iron nitrilotriacetic acid complex, J Chem Soc Dalton Trans, (1993) 3137-3143.
[57] T.E. Adams, A.B. Mason, Q.Y. He, P.J. Halbrooks, S.K. Briggs, V.C. Smith, R.T. MacGillivray, S.J. Everse, The position of arginine 124 controls the rate of iron release from the N-lobe of human serum transferrin. A structural study, J Biol Chem, 278 (2003) 6027-6033.
[58] J.M. El Hage Chahine, R. Pakdaman, Transferrin, a mechanism for iron uptake from nitrilotriacetatoFe(III) in the presence of bicarbonate, J Chim Phys, 93 (1996) 283-299.
[59] M.G. Benavides-Garcia, K. Balasubramanian, Structural insights into the binding of uranyl with human serum protein apotransferrin structure and spectra of protein-uranyl interactions, Chem Res Toxicol, 22 (2009) 1613-1621.
[60] S. Scapolan, E. Ansoborlo, C. Moulin, C. Madic, Uranium speciation in biological medium by means of capillary electrophoresis and time-resolved laser-induced fluorescence, Journal of Radioanal and Nucl Chem, 226 (1997) 145-148.

[61] C. Vidaud, A. Dedieu, C. Basset, S. Plantevin, I. Dany, O. Pible, E. Quemeneur, Screening of human serum proteins for uranium binding, Chem Res Toxicol, 18 (2005) 946-953.
[62] M. Sutton, S.R. Burastero, Uranium(VI) solubility and speciation in simulated elemental human biological fluids, Chem Res Toxicol, 17 (2004) 1468-1480.
[63] J. Michon, S. Frelon, C. Garnier, F. Coppin, Determinations of uranium(VI) binding properties with some metalloproteins (transferrin, albumin, metallothionein and ferritin) by fluorescence quenching, J Fluoresc, 20 (2010) 581-590.
[64] C. Vidaud, S. Gourion-Arsiquaud, F. Rollin-Genetet, C. Torne-Celer, S. Plantevin, O. Pible, C. Berthomieu, E. Quemeneur, Structural consequences of binding of UO2(2+) to apotransferrin: can this protein account for entry of uranium into human cells?, Biochemistry, 46 (2007) 2215-2226.
[65] F. Bou Abdallah, J.M. El Hage Chahine, Transferrins: iron release from lactoferrin, J Mol Biol, 303 (2000) 255-266.
[66] J.C. Dewan, B. Mikami, M. Hirose, J.C. Sacchettini, Structural evidence for a pH-sensitive dilysine trigger in the hen ovotransferrin N-lobe: implications for transferrin iron release, Biochemistry, 32 (1993) 11963-11968.
[67] R.T. MacGillivray, M.C. Bewley, C.A. Smith, Q.Y. He, A.B. Mason, R.C. Woodworth, E.N. Baker, Mutation of the iron ligand His 249 to Glu in the N-lobe of human transferrin abolishes the dilysine "trigger" but does not significantly affect iron release, Biochemistry, 39 (2000) 1211-1216.
[68] N.A. Peterson, V.L. Arcus, B.F. Anderson, J.W. Tweedie, G.B. Jameson, E.N. Baker, "Dilysine trigger" in transferrins probed by mutagenesis of lactoferrin: crystal structures of the R210G, R210E, and R210L mutants of human lactoferrin, Biochemistry, 41 (2002) 14167-14175.
[69] T. Sakajiri, T. Yamamura, T. Kikuchi, K. Ichimura, T. Sawada, H. Yajima, Absence of binding between the human transferrin receptor and the transferrin complex of biological toxic trace element, aluminum, because of an incomplete open/closed form of the complex, Biol Trace Elem Res, 136 (2010) 279-286.
[70] H. Sun, H. Li, A.B. Mason, R.C. Woodworth, P.J. Sadler, Competitive binding of bismuth to transferrin and albumin in aqueous solution and in blood plasma, J Biol Chem, 276 (2001) 8829-8835.
[71] H. Fuchs, R. Gessner, R. Tauber, R. Ghosh, Functional reconstitution of the human placental transferrin receptor into phospholipid bilayers leads to long tubular structures proceeding from the vesicle surface, Biochemistry, 34 (1995) 6196-6207.
[72] D. Sheff, L. Pelletier, C.B. O'Connell, G. Warren, I. Mellman, Transferrin receptor recycling in the absence of perinuclear recycling endosomes, J Cell Biol, 156 (2002) 797-804.
[73] S.P. Young, A. Bomford, R. Williams, The effect of the iron saturation of transferrin on its binding and uptake by rabbit reticulocytes, Biochem J, 219 (1984) 505-510.
[74] A.M. Giannetti, P.J. Bjorkman, HFE and transferrin directly compete for transferrin receptor in solution and at the cell surface, J Biol Chem, 279 (2004) 25866-25875.
[75] A.M. Giannetti, P.M. Snow, O. Zak, P.J. Bjorkman, Mechanism for multiple ligand recognition by the human transferrin receptor, PLoS Biol, 1 (2003) E51.
[76] J.W. Ejnik, T.I. Todorov, F.G. Mullick, K. Squibb, M.A. McDiarmid, J.A. Centeno, Uranium analysis in urine by inductively coupled plasma dynamic reaction cell mass spectrometry, Anal Bioanal Chem, 382 (2005) 73-79.
[77] T.I. Todorov, H. Xu, J.W. Ejnik, F.G. Mullick, K. Squibb, M.M. A., J.A. Centeno, Depleted uranium analysis in blood bu inductively coupled plasma mass spectroscopy, J. Anal. At. Spectrom, 24 (2009) 189-193.

[78] A.P. Turkewitz, J.F. Amatruda, D. Borhani, S.C. Harrison, A.L. Schwartz, A high yield purification of the human transferrin receptor and properties of its major extracellular fragment, J Biol Chem, 263 (1988) 8318-8325.
[79] J.M. El Hage Chahine, R. Pakdaman, Transferrin, a mechanism for iron release, Eur J Biochem, 230 (1995) 1102-1110.
[80] S.L. Byrne, N.D. Chasteen, A.N. Steere, A.B. Mason, The unique kinetics of iron release from transferrin: the role of receptor, lobe-lobe interactions, and salt at endosomal pH, J Mol Biol, 396 (2010) 130-140.
[81] R.W. Evans, J.B. Crawley, R.C. Garratt, J.G. Grossmann, M. Neu, A. Aitken, K.J. Patel, A. Meilak, C. Wong, J. Singh, et al., Characterization and structural analysis of a functional human serum transferrin variant and implications for receptor recognition, Biochemistry, 33 (1994) 12512-12520.
[82] A. Iolascon, L. De Falco, Mutations in the gene encoding DMT1: clinical presentation and treatment, Semin Hematol, 46 (2009) 358-370.
[83] S. Dhungana, C.H. Taboy, O. Zak, M. Larvie, A.L. Crumbliss, P. Aisen, Redox properties of human transferrin bound to its receptor, Biochemistry, 43 (2004) 205-209.
[84] A.T. McKie, A ferrireductase fills the gap in the transferrin cycle, Nat Genet, 37 (2005) 1159-1160.
[85] R.S. Ohgami, D.R. Campagna, E.L. Greer, B. Antiochos, A. McDonald, J. Chen, J.J. Sharp, Y. Fujiwara, J.E. Barker, M.D. Fleming, Identification of a ferrireductase required for efficient transferrin-dependent iron uptake in erythroid cells, Nat Genet, 37 (2005) 1264-1269.
[86] K. Lyczko, A. Bilewicz, I. Persson, Stabilization of a subvalent oxidation state of bismuth in N,N-dimethylthioformamide solution: an EXAFS, UV-Vis, IR, and cyclic voltammetry study, Inorg Chem, 43 (2004) 7094-7100.
[87] T. Privalov, P. Macak, B. Schimmelpfennig, E. Fromager, I. Grenthe, U. Wahlgren, Electron transfer in uranyl(VI)-uranyl(V) complexes in solution, J Am Chem Soc, 126 (2004) 9801-9808.

Figure captions

Figure 1. (A) Fluorescence emission spectra of apotransferrin (T), monoferric transferrin with only an iron-loaded C-lobe (T_CFe) and holotransferrin (TFe_2) in unknown states of protonation and charge with an analytical protein concentration of 2 µM and an excitation maximum (λ_{ex} = 280 nm). (B) Absorption spectra of T, T_CFe and T_CFe_2 between 400 and 550 nm. Absorption and emission are reported at 25 °C and µ = 0.2 [28, 79].

Figure 2. Schematic view of a stopped flow-spectrometer equipped with spectrophotometric detection. The two drive syringes are filled via the T-valves with the two solutions in reservoirs A and B. A pneumatic device is used to push the two pistons of the syringes A and B to rapidly drive the two solutions into the mixing chamber. The mixing chamber is transparent to light, which allows the use of a spectrophotometer either in emission or absorption. The flow coming from the mixing chamber is directed to the stop syringe where it drives the stop piston to the triggering device, which interrupts the flow and starts the acquisition. Mixing time occurs in the millisecond range.

Figure 3. Normalized variation in the fluorescence emission with time after fast mixing of solutions of transferrin and FeNTA, which shows iron transfer from the FeNTA chelate to apotransferrin, reported for an excitation wavelength (λ_{ex} = 280 nm), an emission wavelength (λ_{em} > 300 nm), at 25 °C and µ = 0.2. A) Fast iron-transfer to the C-lobe in the open conformation to yield a first kinetic intermediate; B) two proton losses triggered conformational change of the first kinetic intermediate; C) a third proton loss triggered conformational change; D) slow final change in the conformation during which an iron is transferred from a second chelate to the N-lobe and the protein attains its final closed conformation [15, 32].

Figure 4. Variations in the normalized emission (A, B) and differential absorption (C) with time, after fast mixing of solutions of apotransferrin and uranyl tricarbonate, show uranyl transfer from the uranyl tricarbonate to apotransferrin, reported for λ_{ex} = 280 nm, λ_{em} > 300 nm at 25 °C for μ = 0.2. A) Uranyl dicarbonate transfer to the C-lobe yielding a first kinetic product; B) conformational change in the first kinetic product leading to the loss of a bicarbonate from the ternary complex intermediate; C) final slow conformational change of the second intermediate, during which an uranyl is transferred to the N-lobe [12].

Figure 5. Schematic view of a T-jump spectrometer equipped with spectrophotometric detection in absorption and/or emission. The high voltage generator (0 – 40 kV) is used to charge a capacitor (0.01 – 0.05 μF). The capacitor is then discharged via the spark gap into the T-jump cell between two platinum electrodes. Heating occurs by the Joule effect in 0.2 – 5 μs and depends on the size of the capacitor and the impedance of the solution. Triggering and acquisition are controlled by the discharge of the capacitor.

Figure 6. Variation of the normalized absorbance (A and insert in C) and fluorescence emission with time during cobalt transfer from the $CoNTACO_3^{2-}$ mixed complex to transferrin, reported at 25 °C and μ = 0.2. (A) Cobalt carbonate transfer to the C-lobe, detected by a fast T-jump from 15 to 25 °C; (B) conformational changes triggered by two proton losses to yield a second kinetic product; (C) Two final conformational changes during which the N-lobe of becomes cobalt-loaded [11].

Figure 7. Schematic view of the interaction between holotransferrin and receptor 1, which occurs in the two steps reported in Figure 8. The first step is the very fast (50 μs) interaction of the C-lobe of holotransferrin with the helical domain of the receptor to yield a first kinetic intermediate. The second step is the very slow (2 hours) change in

the conformation of the protein/protein adduct intermediate to yield the thermodynamic species in which the N-lobe becomes in interaction with the protease-like domain of the receptor [13].

Figure 8. Variation of the normalized fluorescence emission with time: A) after a T-jump from 25 to 37 °C performed on solutions of TFe_2, TGa_2, TBi_2, TCo_2 in the presence of receptor 1; (B) after stopped-flow mixing of solutions of TUr_2 and TFR; (C) and (D) at the end of the fast kinetic processes in (A) and (B) for TFe_2, TCo_2 and TUr_2 recorded with λ_{ex} = 280 nm and λ_{em} > 300 nm at 37 °C and μ = 0.2. All spectra were acquired in the presence of 1 mM of CHAPS and μ = 0.2 [10-11, 13-14, 47].

Figure 9. Iron release from holotransferrin upon interaction with receptor 1 occurs in three distinctive kinetic steps. (A) The first is fast and detected when the pH-jump from a neutral to an acidic medium is achieved by stopped-flow mixing. It occurs as an exponential increase in the emission, describing iron release from the N-lobe of transferrin upon interaction with the receptor. (B) The second is also an increase in emission, describing iron loss from the C-lobe upon interaction with the receptor. (C) The third appears as a slow decrease in emission (about 20 minutes) during which an equilibrium is achieved between the free acidic form of the receptor and that upon interaction with apotransferrin. All kinetic runs were recorded with λ_{ex} = 280 nm for λ_{em} > 300 nm at 37 °C and μ = 0.2 [13, 16].

Figure 10. The mechanism of iron transport from the blood serum to cytosol: The C-lobe of holotransferrin interacts instantaneously (50 μs) with the helical domain of the receptor, whereas the interaction of the N-lobe is very slow (2 hours). Statistically, transferrin will thus be internalized mainly with the C-lobe interacting with the receptor. After acidification of the endosome, iron is released in the cytosol within seconds. This release is much faster than endocytosis. In vitro, apotransferrin is partly

released from the protein adduct formed by its interaction with acidic form of the receptor within 20 minutes, which is longer than the recycling time of the endosome to the cell surface. This implies the recycling of a transferrin mainly upon interaction with the acidic receptor. In neutral media, the neutral form of the receptor loses its affinity for apotransferrin, which breaks the protein/protein adduct releasing transferrin into the serum [13, 16].

Reaction		Direct rate constant	Reverse rate constant	Dissociation constant
Iron transfer				
$T'_CH_2 + HCO_3^- \rightleftharpoons T_CH_3$	(1)			4.35 mM
$T_CH_3 + FeL' \rightleftharpoons T_C H_3Fe + L$	(3)	$8.0X\ 10^4\ M^{-1}\ s^{-1}$	$7.5 \times 10^4\ M^{-1}\ s^{-1}$	1.00
$T_CH_3\ Fe \rightleftharpoons T_CH_2Fe + H^+$	(3)			16 nM
$H_3T_NT_CH_2Fe \rightleftharpoons TH_5Fe$	(4)	$2.80\ s^{-1}$		
$TH_5Fe \rightleftharpoons TH_{(5-l)}Fe + lH^+$	(5)			
$T'H_{(5-m)}Fe \rightleftharpoons TH_{(5-l)}Fe$	(6)	$6.2 \times 10^{-2}\ s^{-1}$		
$T'H_{(4-m)}Fe + H^+ \rightleftharpoons T'H_{(5-l)}Fe$	(7)			6.8 nM
$T'H_{(4-m)}Fe \rightleftharpoons T"H_{(4-l)}Fe$	(8)			
$T'H_{(4-m)}Fe_2 \rightleftharpoons T"H_{(4-l)}Fe_2$	(9)			
$T'H_{(4-m)}Fe + FeL \rightleftharpoons L + T'H_{(4-l)}Fe_2$	(10)			
$T_CH_3 + Fe^{3+} \rightleftharpoons T_CH_3Fe$	(11)			$\sim 1 \times 10^{-16}$ M
Aluminum transfer				
$T_CH_3 + AlL \rightleftharpoons T_CH_3Al + L$	(12)	$(44 \pm 3)\ M^{-1}\ s^{-1}$	$(2.3 \pm 0.6) \times 10^3\ M^{-1}\ s^{-1}$	$(2.0 \pm 0.6) \times 10^{-2}$
$T_C H_3Al \rightleftharpoons T_CH_2Al + H^+$	(13)			(15.0 ± 3) nM
$H_jT_NT_CH_2Al \rightleftharpoons TH_{j+2}Al$	(14)	$(4.20 \pm 0.02) \times 10^{-2}\ s^{-1}$		
$TH_jAl + 2H^+ \rightleftharpoons TH_jAl$	(15)			
$TH_jAl \rightleftharpoons T' H_jAl$	(16)			
$T'H_jAl + AlL \rightleftharpoons L + T'H_jAl_2$	(17)			
$T'H_jAl_2 \rightleftharpoons T"H_jAl_2$	(18)			
$T_CH_3 + Al^{3+} \rightleftharpoons T_CH_3Al$	(19)			~ 35 nM
Bismuth transfer				
$T_CH_3 + BiL \rightleftharpoons T_CH_3Bi + L$	(20)	$(2.45 \pm 0.20) \times 10^5\ M^{-1}\ s^{-1}$	$(1.5 \pm 0.5) \times 10^6\ M^{-1}\ s^{-1}$	(6 ± 4)
$T_C H_3Bi \rightleftharpoons T_CH_2Bi + H^+$	(21)			(2.4 ± 0.10) nM
$H_jT_NT_CH_2Bi \rightleftharpoons TH_{j+2}Bi$	(22)	$25 \pm 1.5\ s^{-1}$		
$TH_jBi + 2H^+ \rightleftharpoons TH_jBi$	(23)			
$TH_jBi \rightleftharpoons T' H_jBi$	(24)			
$T'H_jBi + BiL \rightleftharpoons L + T'H_jBi_2$	(25)			
$T'H_jBi_2 \rightleftharpoons T"H_jBi_2$	(26)			

$T_CH_3 + Bi^{3+} \rightleftharpoons T_CH_3Bi$	(27)			$(1.5 \pm 1) \times 10^{-17}$ M
Gallium transfer				
$T_CH_3 + GaL \rightleftharpoons T_CH_3Ga + L$	(28)	450 M^{-1} s^{-1}	11000	3.9×10^{-2}
$T_CH_2Ga + H^+ \rightleftharpoons T_CH_3Ga$	(29)			80 nM
$T_CH_3Ga \rightleftharpoons T_CGa$	(30)			
$T_CGa \rightleftharpoons$ Unknown	(31)			
Unknown $GaL + (mH^+)? \rightleftharpoons TGa_2$				

Table 1 The mechanisms of metal exchange between a chelate and transferrin where TCH_3 is the C-lobe of apotransferrin with bound HCO_3^- in neutral media but with unknown charge, L is the chelator, NTA and AHA for Fe(III), NTA for Ga(III) and Bi(III) and citrate for Al(III), TFe_2, TAl_2, TBi_2 and TGa_2 are iron-, aluminum-, bismuth- and gallium-saturated transferrins in their final thermodynamic states [4, 10, 14-15, 32].

Uranyl uptake by transferrin		Direct rate constant	Reverse rate constant	Equilibrium constant
$Ur(CO_3)_3^{4-} + H^+ \rightleftharpoons Ur(CO_3)_2^{2-} + HCO_3^-$	(32)			0.46 µM
$Ur(CO_3)_3^{4-} + T_C \rightleftharpoons (T_CUr(CO_3)_2)' + HCO_3^-$	(33)	$7.4 \times 10^5\ M^{-1}\ s^{-1}$	$4.6 \times 10^3\ M^{-1}\ s^{-1}$	6.3 mM
$(T_CUr(CO_3)_2)'' \rightleftharpoons (T_CUr(CO_3)_2)'$	(34)	$33\ s^{-1}$	--------	
$T_CUr + HCO_3^- \rightleftharpoons (T_CUr(CO_3)_2)''$	(35)			
$T_CUr \rightleftharpoons \underset{\overset{+}{?\ H}}{\underline{\text{unknown}}} \rightleftharpoons TUr_2$ ($Ur(CO_3)_3^{4-}$)	(36)			
Cobalt uptake				
$T_CH_m + CoNtaCO_3^{2-} \rightleftharpoons T_CH_mCoCO_3 + Nta^{3-}$	(37)	$1.1 \times 10^6\ M^{-1}\ s^{-1}$	$1.9 \times 10^6\ M^{-1}\ s^{-1}$	1.7
$T_CH_{m-1}CoCO_3 + H^+ \rightleftharpoons T_CH_mCoCO_3$	(38)			6 nM
$T_CH_{m-2}CoCO_3 + H^+ \rightleftharpoons T_CH_{m-1}CoCO_3$	(39)	$2.9 \times 10^6\ M^{-1}\ s^{-1}$	$1.6 \times 10^{-2}\ s^{-1}$	6.2 nM
$T_CH_{m-2}CoCO_3 \rightleftharpoons \underset{?\ H^+}{\underline{\text{unknown}}} \rightleftharpoons TCo_2$ ($CoNtaCO_3^{2-}$)	(40)			

Table 2. The mechanisms of uranyl and cobalt uptake by transferrin with T_C, and The C-lobe of serum transferrin in unknown states of protonations and charges; TUr_2 and TCo_2, uranyl- and cobalt-saturated transferrins in the final state of equilibrium [11, 47].

Reaction	Direct rate constant	Reverse rate constant	Equilibrium constant	Affinity constants
TFR + H^+ ⇌ TFRH (41)			10 nM	1 X 10^8 M^{-1}
Iron-saturated transferrin				
TFR + TFe_2 ⇌ $TFRTFe_2$ (42)			2.3* and 0.6 nM	43.5* and 1.7 X 10^9
TFR + TFe_2 ⇌ $(TFRTFe_2)'$ (43)	3.2 x 10^{10} M^{-1} s^{-1}	1.6 x 10^4 s^{-1}	0.5 µM	2 X 10^6 M^{-1}
$(TFR\text{-}TFe_2)'$ ⇌ $TFRTFe_2$ (44)			4.6 X 10^{-3}	217
Interaction with HFE				
TFR + HFE ⇌ TFRHFE (45)			24 nM	4.17 X 10^7 M^{-1}
Cobalt-saturated transferrin				4 X 10^7 M^{-1}
TFR + TCo_2 ⇌ $(TFRTCo_2)'$ (46)	4.4 X 10^{10} M^{-1} s^{-1}	3.6 X 10^4 s^{-1}	0.8µM	1.25 X 10^6 M^{-1}
$(TFRTCo_2)'$ ⇌ $TFRTCo_2$ (47)			3 X 10^{-2}	33
TFR + TCo_2 ⇌ $TFRTCo_2$ (48)			25 nM	4 X 10^7 M^{-1}
Gallium-saturated transferrin				
TFR + TGa_2 ⇌ $TFRTGa_2$	1.15 X 10^{10} M^{-1} s^{-1}	1.3 s^{-1}	1.1 µM	9.1 X 10^5 M^{-1}
Bismuth-saturated transferrin				
TFR + TBi_2 ⇌ $TRF\text{-}TBi_2$ (49)	2.2 X 10^8 M^{-1} s^{-1}	900 s^{-1}	4 µM	2.5 x 10^5 M^{-1}
Uranyl-saturated transferrin				
TFR + TUr_2 ⇌ $(TFR\text{-}TUr_2)$ (50)	5.2 x 10^6 M^{-1} s^{-1}	95 s^{-1}	18 µM	5.6 x 10^4 M^{-1}
$(TFR\text{-}TUr_2)$ ⇌ $TFR\text{-}TUr_2$ (51)			0.3	3
TFR + TUr_2 ⇌ $TFR\text{-}TUr_2$ (52)			6 µM	1.7 x 10^5 M^{-1}

Table 3. The mechanisms of interaction of iron-, cobalt-, gallium- bismuth- uranyl- saturated transferrins and HFE with a receptor 1 subunit [10-14, 74].

Reaction	Second order rate constant (M^{-1} s^{-1})	first order rate constant (s^{-1})	Equilibrium constant
$T_NFeTFR + H^+ \rightleftharpoons HT_NFeTFR + CO_2$ (56)			
$HT_NFeTFR + H^+ \rightleftharpoons H_2T_NFeTFR$ (57)	$(1.20 \pm 0.05) \times 10^6$		
$H_2T_NTFR + Fe^{3+} \rightleftharpoons H_2T_NFeTFR$ (58)			
$H_2T_NTFR + 2H^+ \rightleftharpoons H_4T_NFeTFR$ (59)			$(2.80 \pm 0.28) \times 10^{-11}$ M^2
$T_CFeTFR + H^+ \rightleftharpoons HT_CFeTFR + CO_2$ (60)	(2.25×10^4) *(15)*		
$HT_CFeTFR + H^+ \rightleftharpoons H_2T_CFeTFR$ (61)	$(1.60 \pm 0.12) \times 10^3$		
$H_2T_CTFR + Fe^{3+} \rightleftharpoons H_2T_CTFR$ (62)			
$H_2T_CTFR + 2H^+ \rightleftharpoons H_4T_CTFR$ (63)			$(6.4 \pm 0.6) \times 10^{-11}$ M^{-2}
$TFRH \rightleftharpoons TFRa + H^+$ (53)			$(2.6 \times 10^{-6}$ M)
$TFR_a \rightleftharpoons TFR_a'$ (54)		$(1.65 \pm 0.05) \times 10^{-3}$	
$TFR_a' + TH_6 \rightleftharpoons TFR'_a\text{-}TH_6$ (55)			
$TFR'a + TH_6 \rightleftharpoons \cdots \rightleftharpoons TH_6TFR$ (57)			$(3.6 \times 10^{-8}$ M)
$Fe^{3+} + L \rightleftharpoons FeL$ (64)			$(4 \times 10^{-4}$ M)

Table 4. The mechanism of iron-release from the $TFRTFe_2$ adduct in acidic media ($4.5 \leq pH \leq 6$) where T_N, is N-lobe, T_C, is the C-lobe, TH_6, is transferrin with all the protein ligands protonated [16].

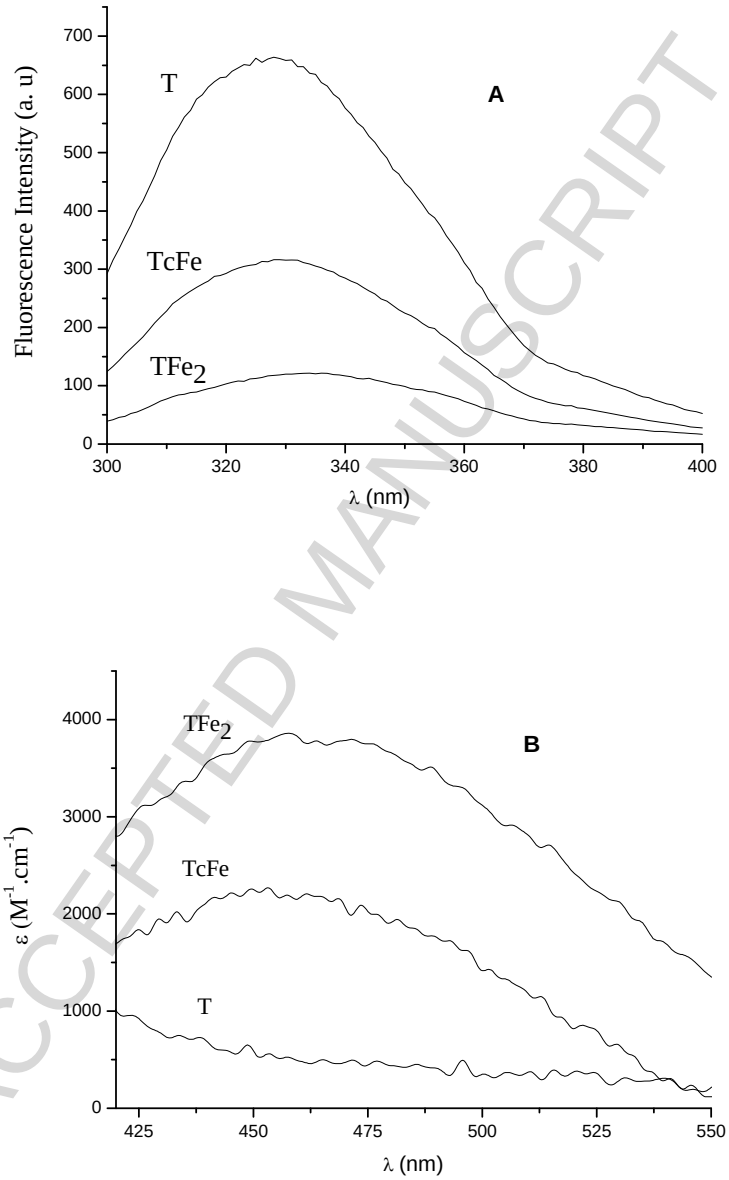

Figure 1

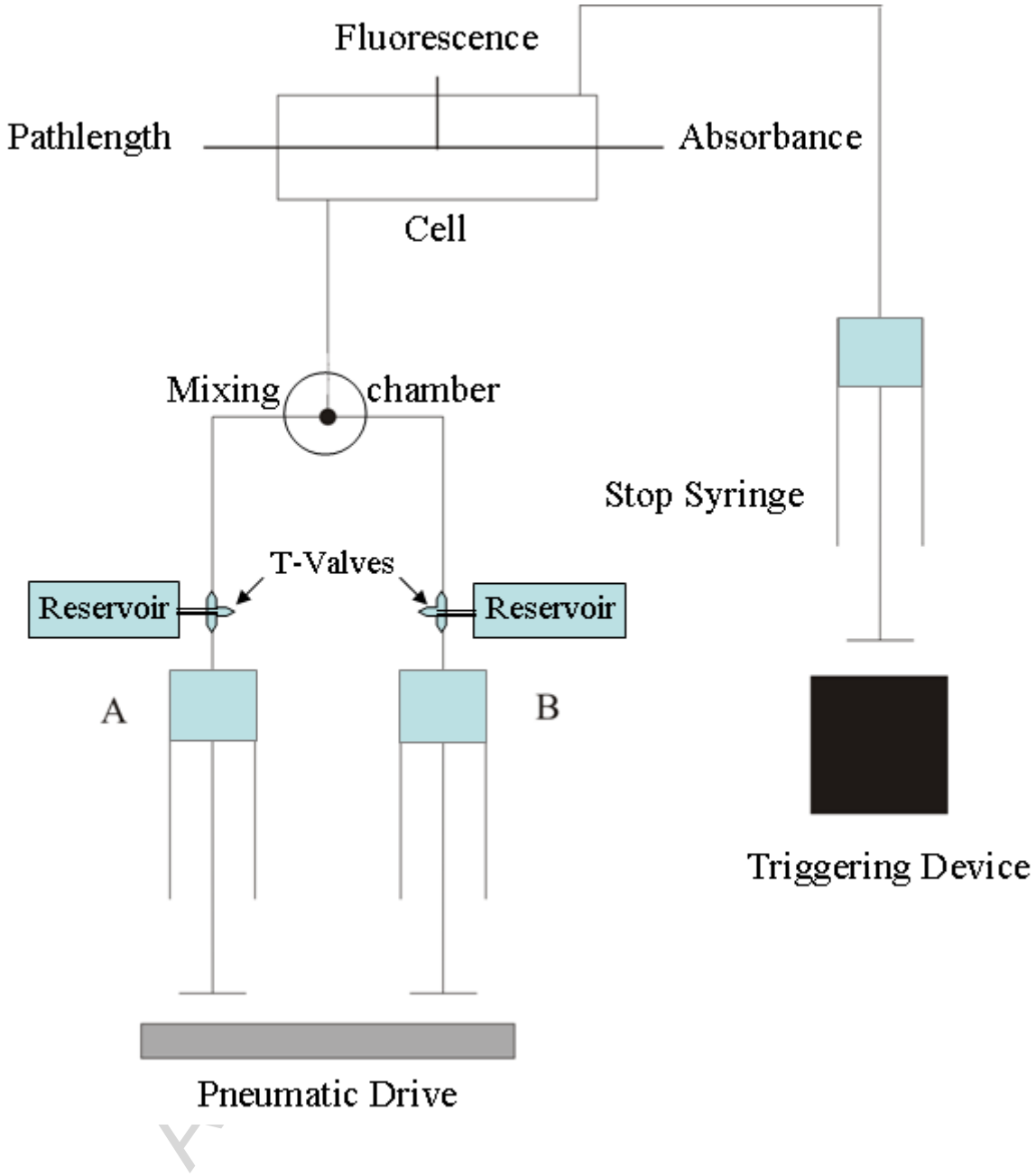

Figure 2

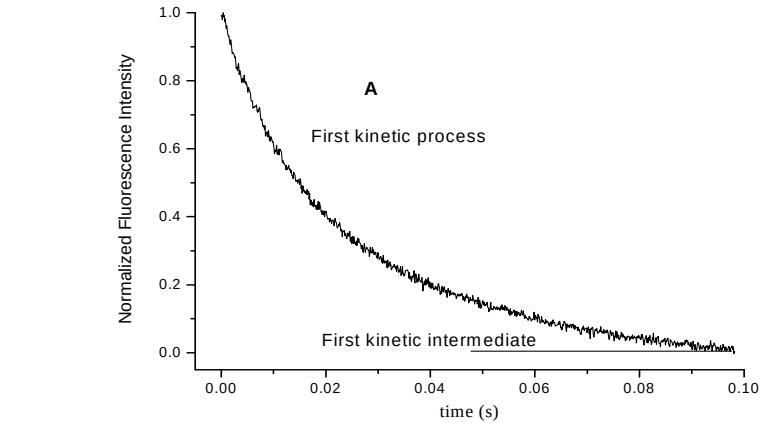

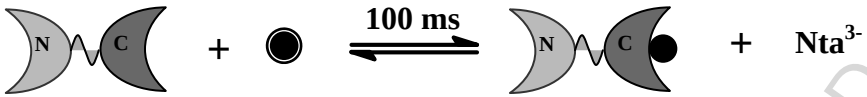

FeNta

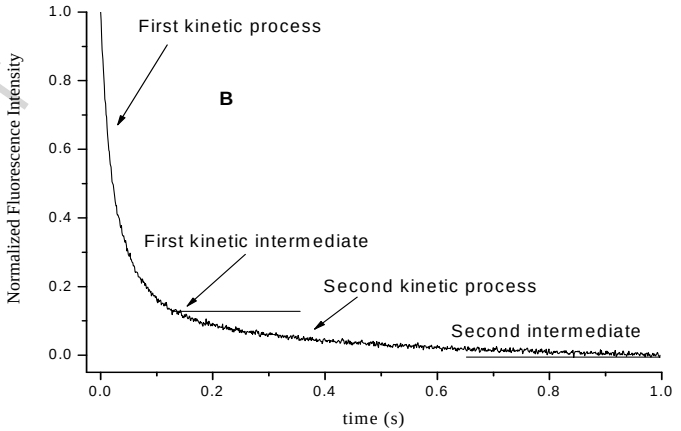

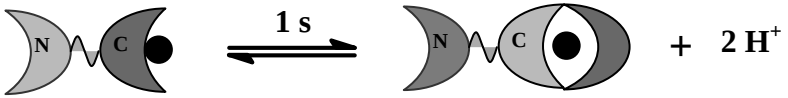

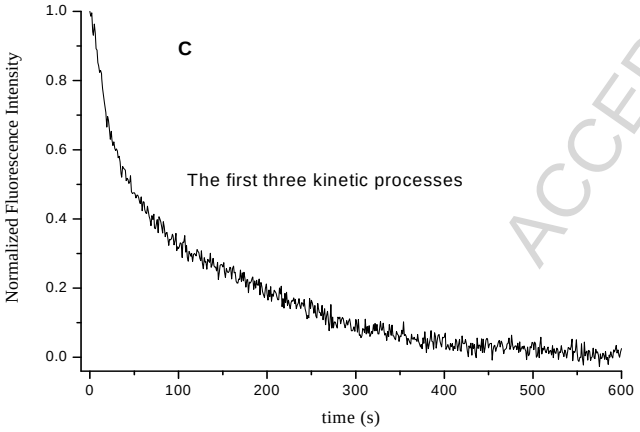

Figure 3

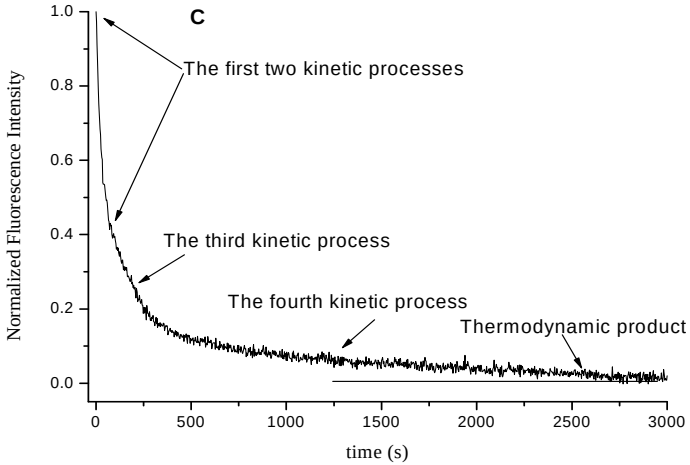

TFe_2

Figure 4

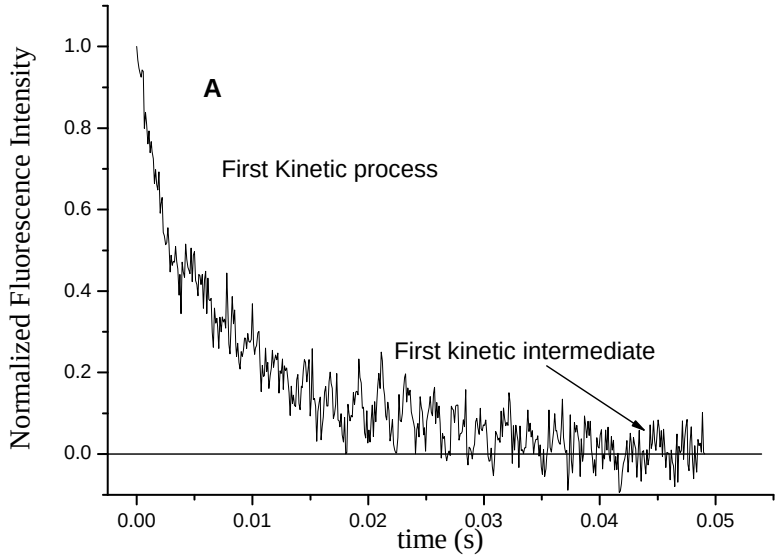

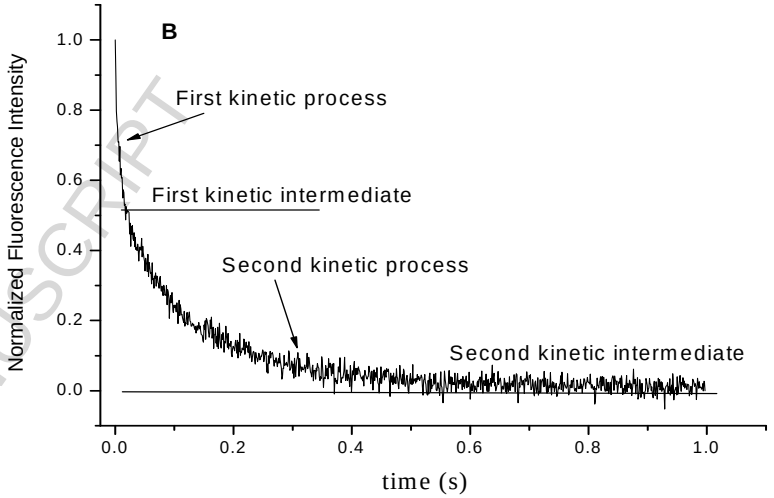

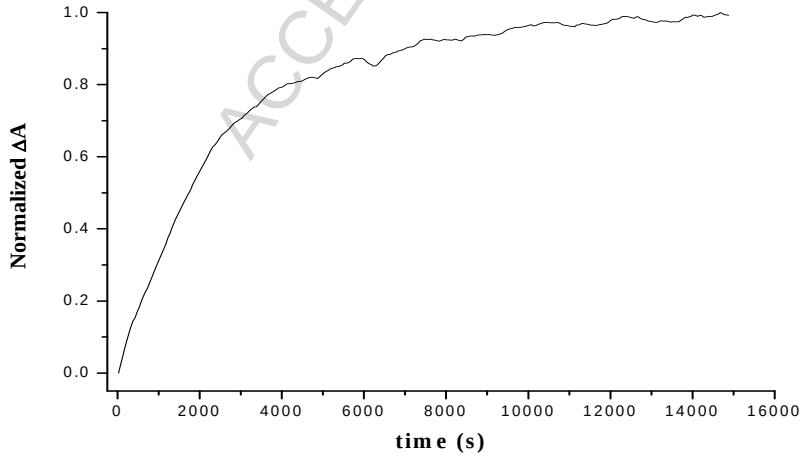

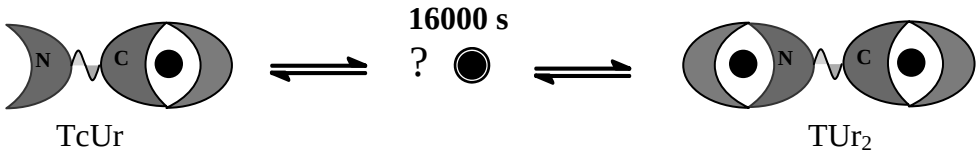

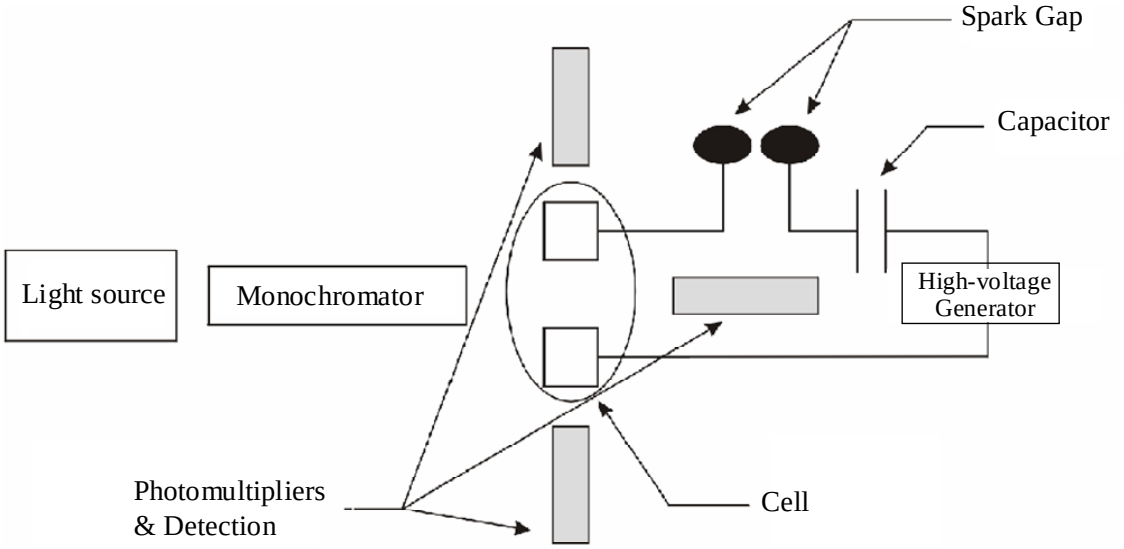

Figure 5

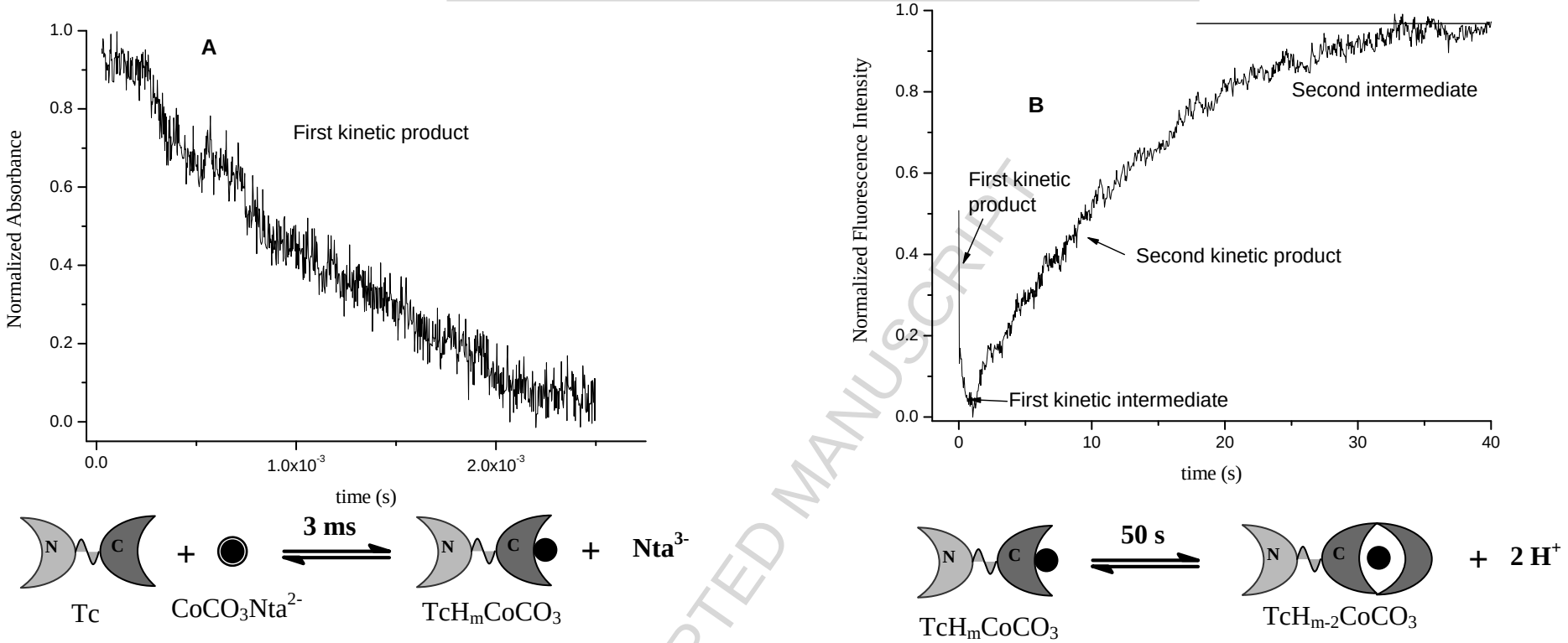

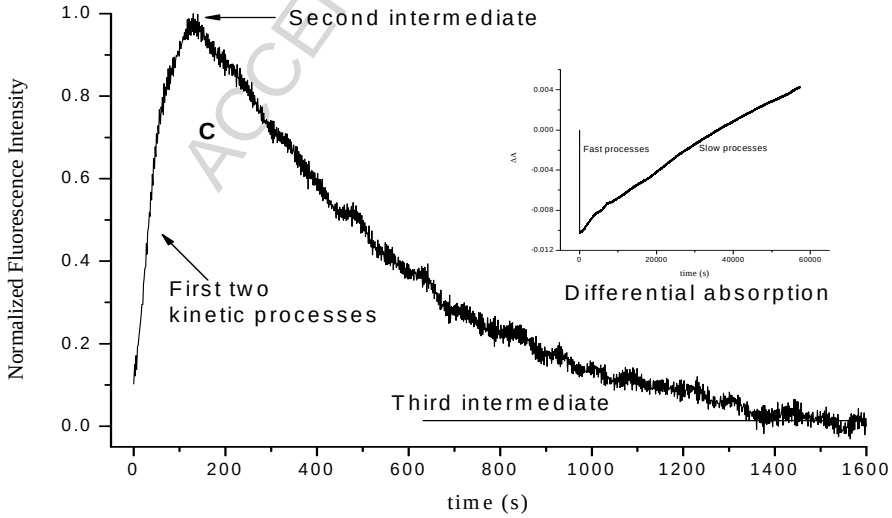

Figure 6

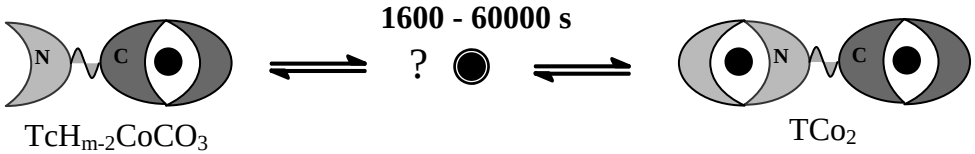

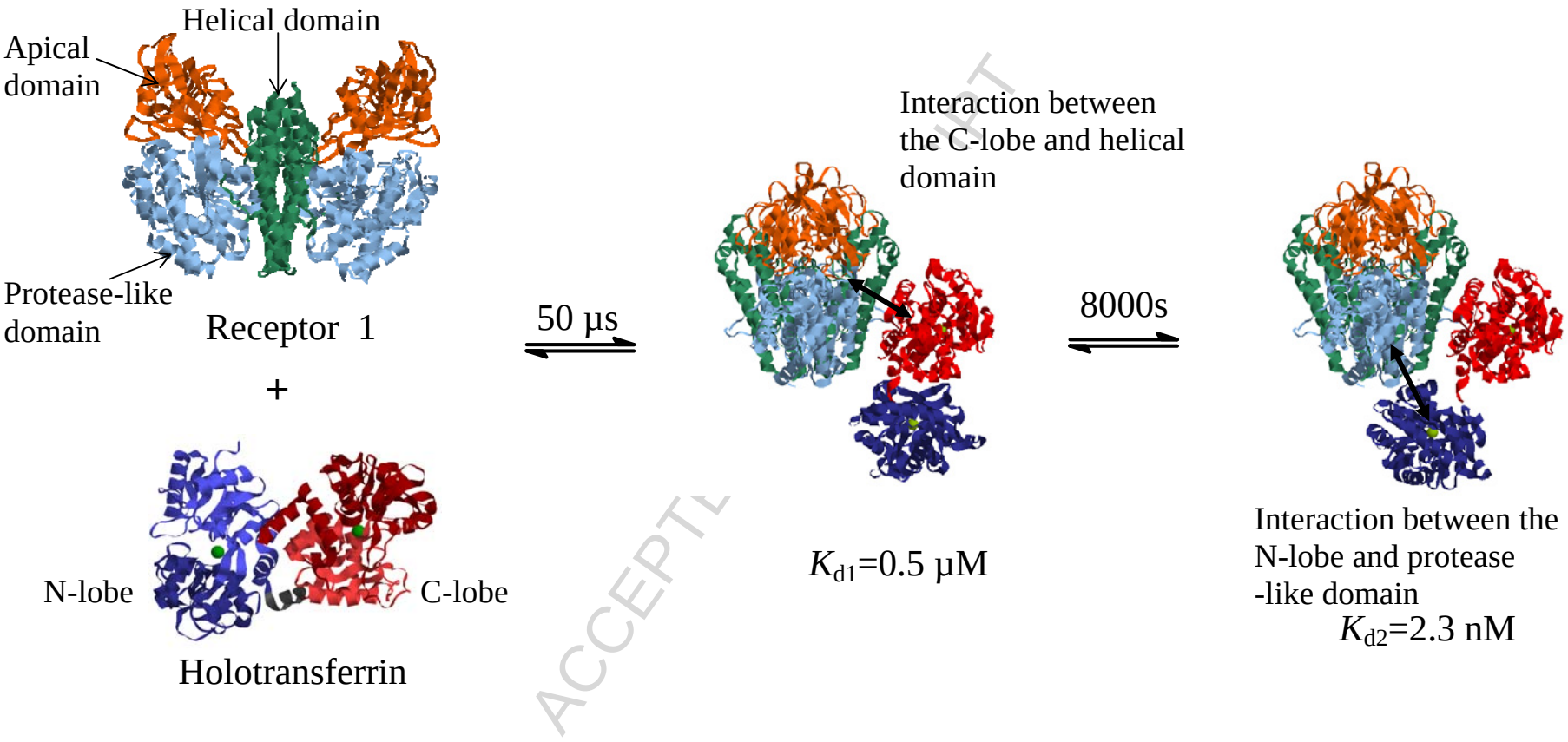

Figure 7

Figure 8

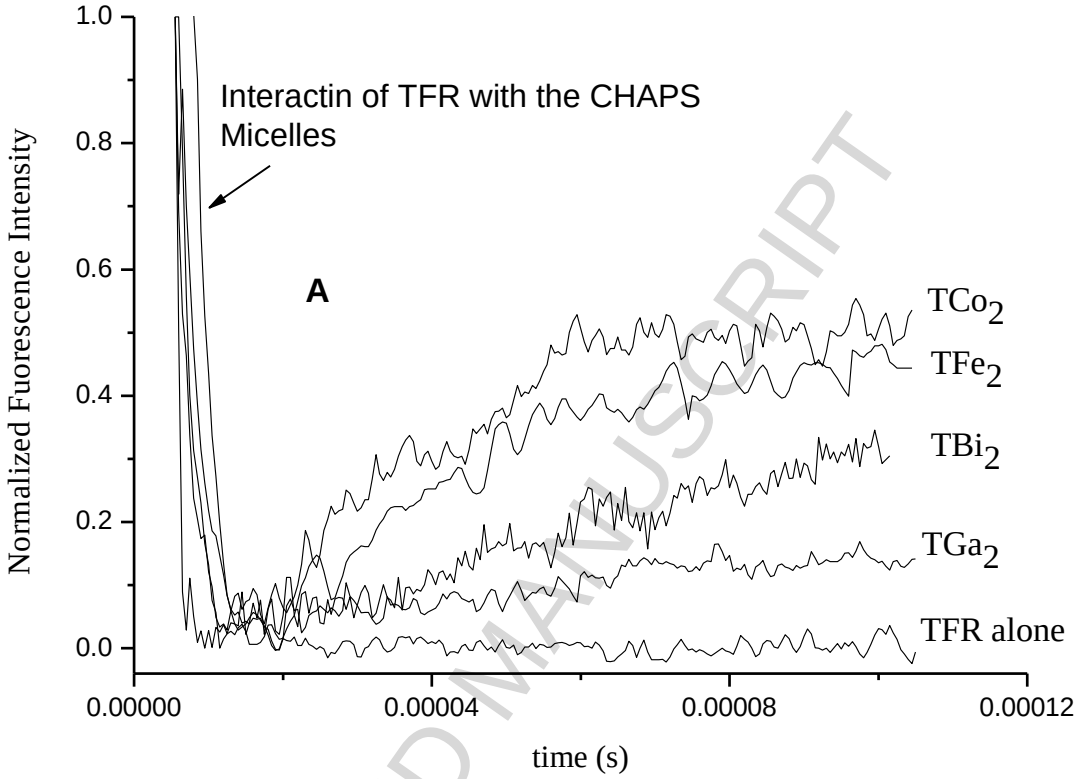

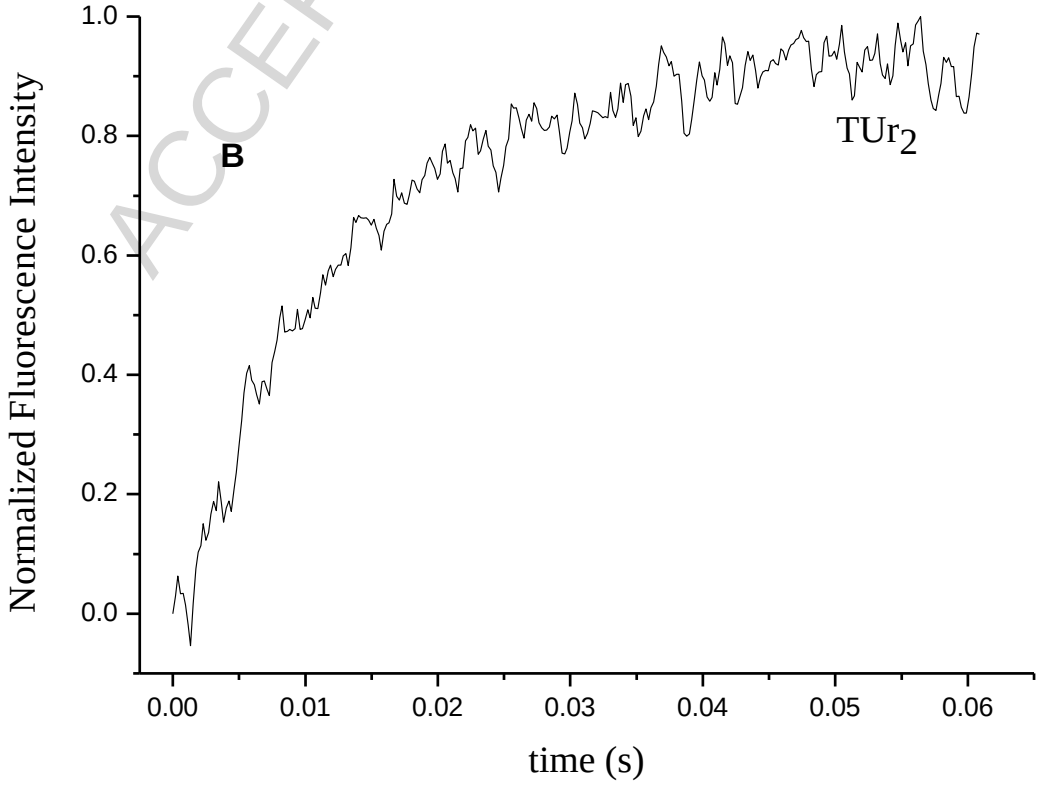

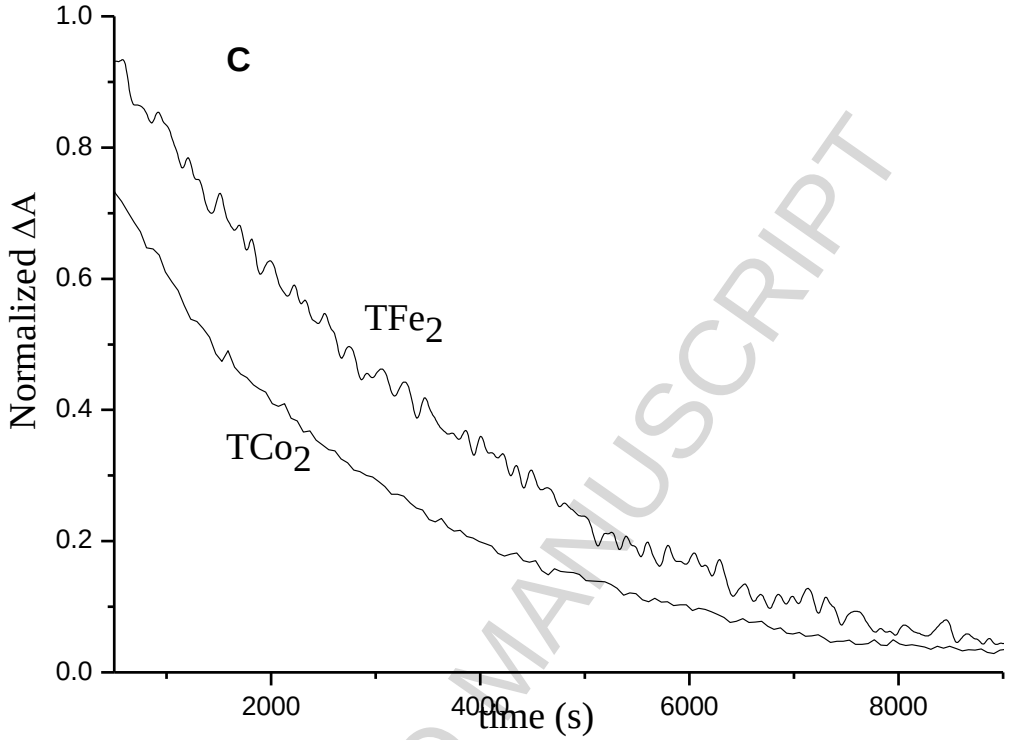

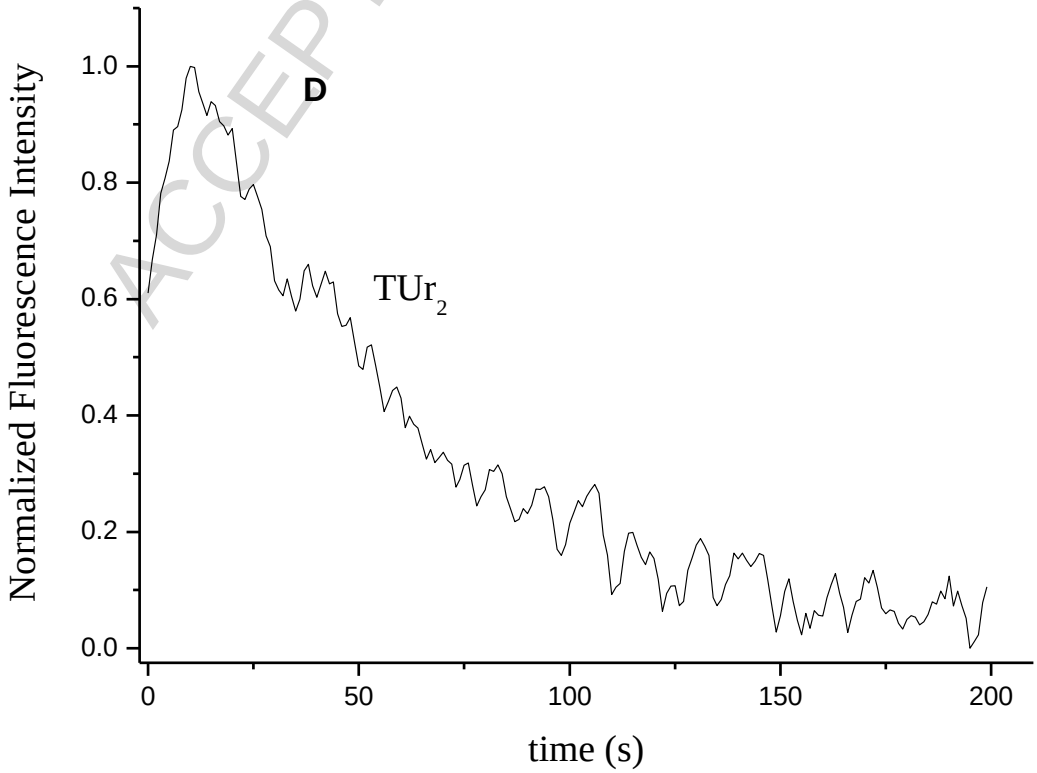

Figure 9

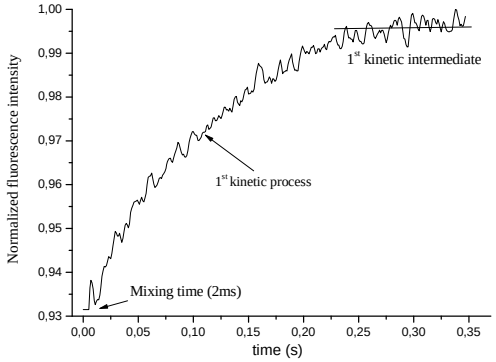

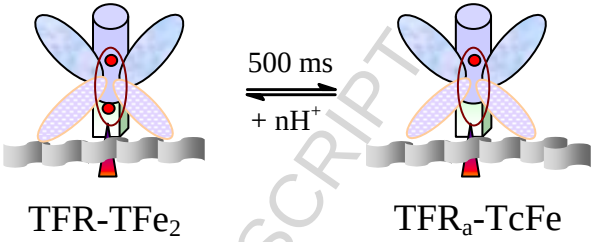

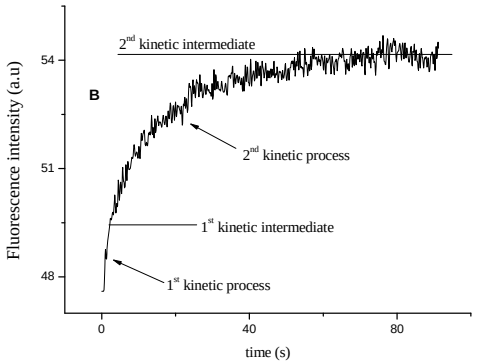

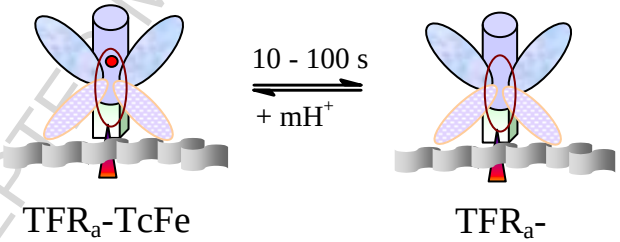

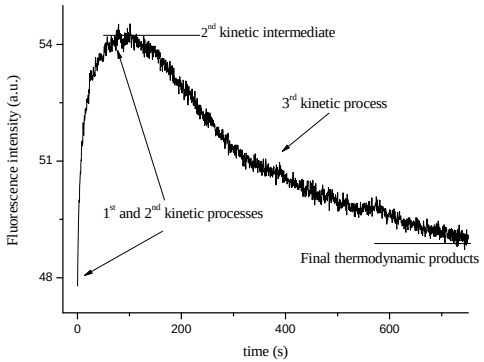

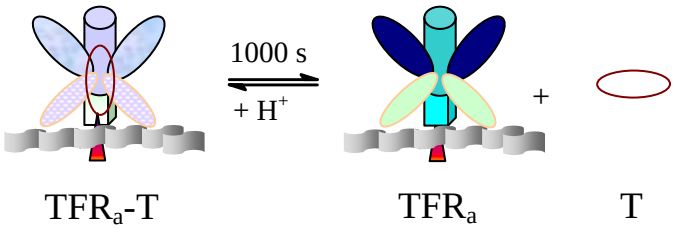

Figure 9

Figure10

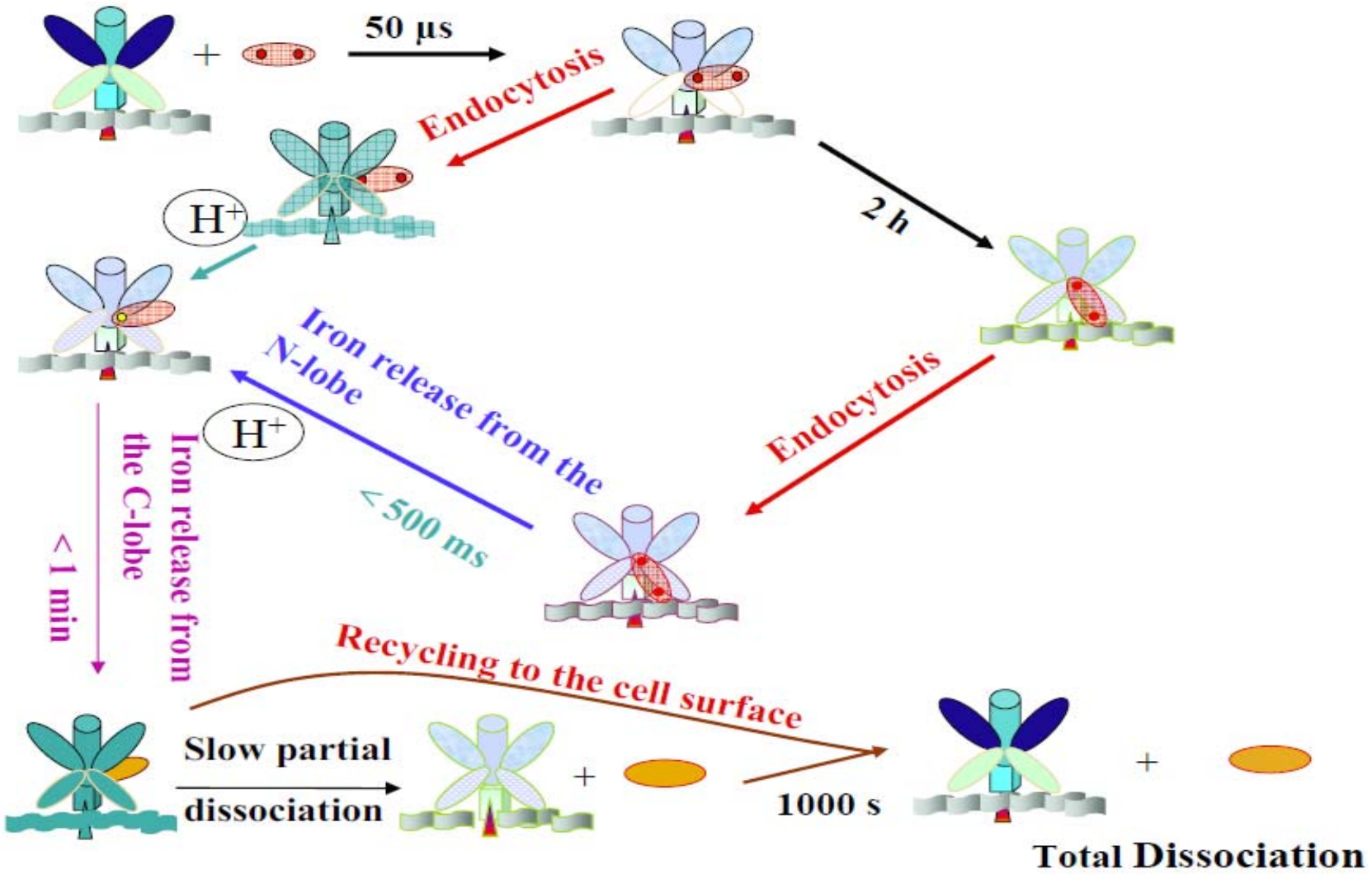

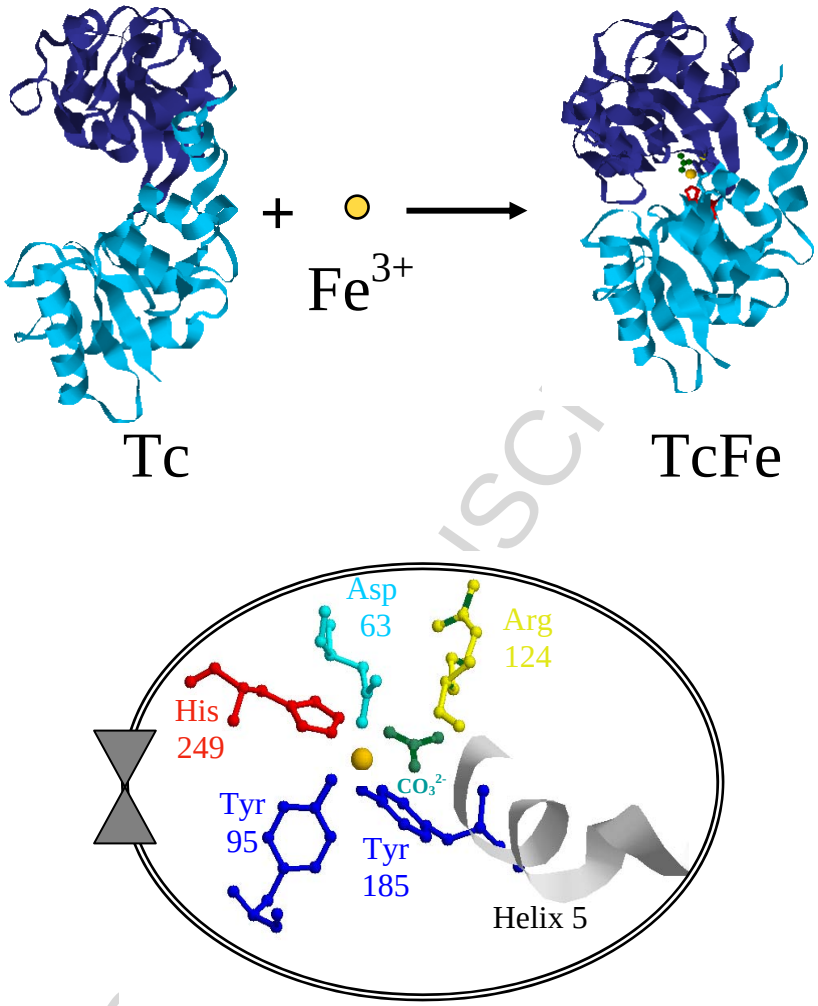

Scheme I. A ribbon representation of the open and closed-structure of the C-lobe of transferrin and a schematic view of the iron complex [18].

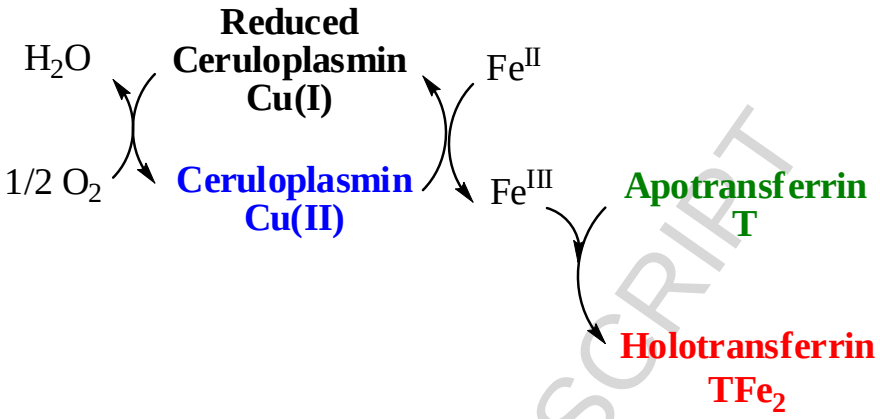

Scheme II. The oxidation of Fe(II) into Fe(III) in ceruloplasmin upon interaction with apotransferrin and its eventual transfer to transferrin [26].